Laser Operational Periods: ICESat/GLAS Data

TABLE OF CONTENTS

1 ATTRIBUTES

The NASA ICESat/GLAS instrument has three lasers, each of which has a 1064 nm laser channel for surface altimetry and dense cloud heights, and a 532 nm lidar channel for the vertical distribution of clouds and aerosols. The three lasers have been operated one at a time, sequentially throughout the mission. To extend mission life, the operational mode included 33-day to 56-day campaigns, several times per year.

A metadata table, *Attributes for ICESat Laser Operations Periods*, provided by the ICESat Science Investigator-led Processing System (I-SIPS), was created in an effort to better educate ICESat/GLAS users on the vertical and horizontal accuracies of the data as well as to provide important information on the laser operating periods and data releases. This table, presented in Appendix A: NSIDC Distributed ICESat GLAS Laser Operations Periods: Latest Release, is a single source for much of the important data related to these operational campaigns, and it includes:

- Laser transmit energies for the two wavelengths
- Laser footprint size and shape
- Pointing and geolocation accuracies

NOTE: References to GLAS binary product names GLA01 to GLA15, refer to original GLAS binary data, and are retained here for informational and provenance purposes. Access to GLAS binary data was removed 01 August, 2017. All GLAS data are available in HDF5 format, products GLAH01 to GLAH15.

Please see the YXX Release Numbers web page for information about a new convention for release numbers in file names that was adopted with Release-28.

The ICESat satellite operated in two attitude modes called “airplane” and “sailboat” which were named for the respective orientation of the satellite's solar arrays. Depending on the position of the spacecraft's orbital plane and the Sun, the satellite's attitude was changed from airplane to sailboat to accommodate sun angle changes and for power and thermal stability. For more information, see section 3, ICESat Attitudes.

2 PERIODS AND COVERAGE

ICESat operational periods are summarized in the Table 1 below (courtesy of Christopher A. Shuman, University of Maryland Baltimore County Goddard Earth Sciences and Technology Center, and Vijay P. Suchdeo, Sigma Space at NASA/GSFC).

2.1 ICESat World and Polar Elevation Maps 2003-2009

To facilitate visualization of the temporal and spatial coverage of ICESat elevation data, please refer to the World and Polar maps in Appendix B: Icesat World Maps 2 and Appendix C: Icesat Polar Maps 2. These files show elevations from the original binary GLA06 elevation data product at two resolutions, browse and high, although it is not possible to show all the detail in the actual data sets. The appendices provide a series of sequential images.

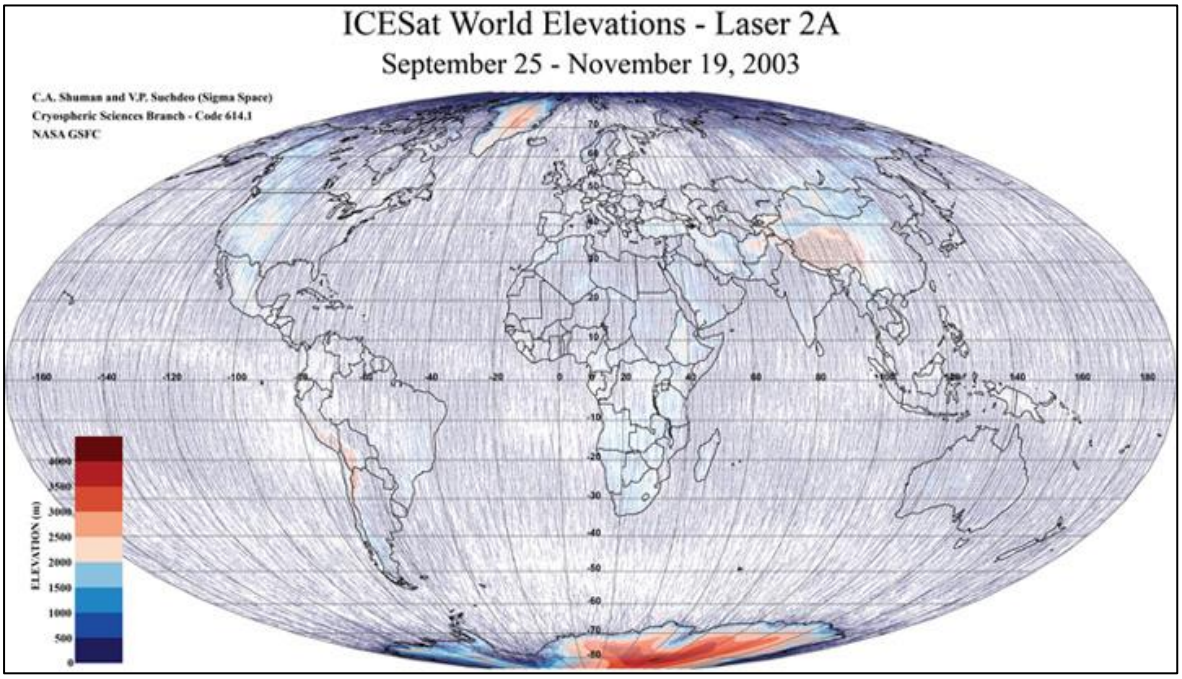

Figure 1. Sample ICESat World Elevation Map

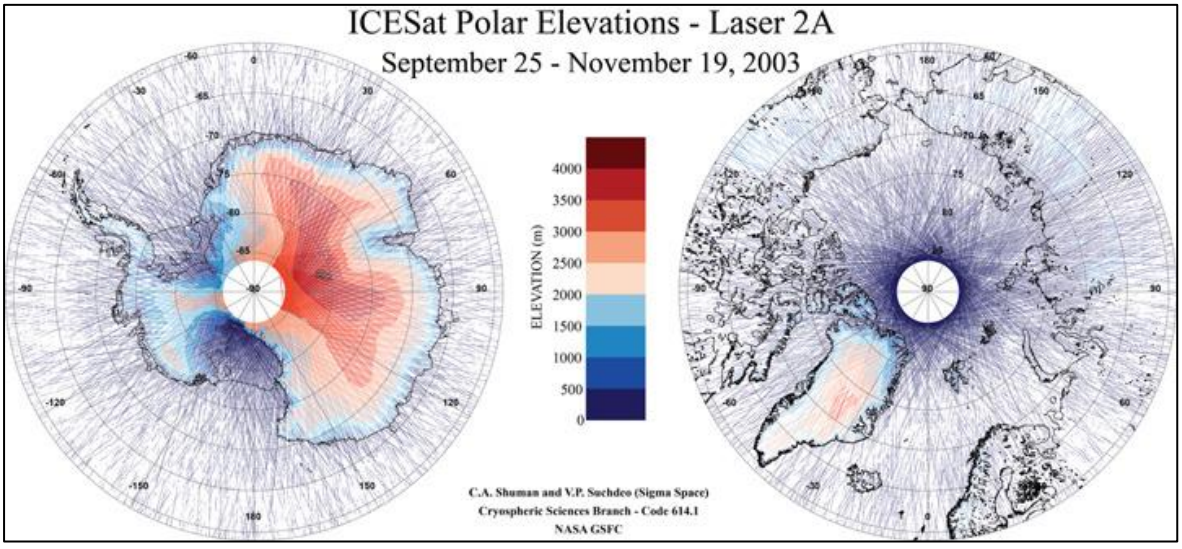

Figure 2. Sample ICESat Polar Elevation Maps

For each elevation map, the lowest elevations, sea level to 500 meters, are shown in dark blue, and the other colors define higher elevations in 500-meter increments. See the scale bars on the maps. All elevations above 4000 meters are represented by a dark red color. Note the relative scale of the polar ice sheets compared to other global, high-elevation land areas; the map projection causes some areal distortion but it is apparent that few other topographic features are as high and wide as the Greenland and Antarctic ice sheets.

White spaces on each of the maps are areas where no elevation data were obtained. This includes gaps along any individual track, generally due to atmospheric losses, as well as between adjacent tracks due to ICESat's 8-day and partial 91-day sampling patterns which both converge at ~86° N and S latitude. In some campaigns the track pattern can be locally distorted, in some cases due to off-nadir pointing of the GLAS laser altimeter. Laser performance variations over the mission life time also impact temporal and spatial coverage of elevation data (see mission calendars). For more information, contact NSIDC User Services.

Table 1. ICESat Operational Periods and Laser ID

Start Date	End Date	Days in Operation	Laser Identifier
2003-02-20	2003-03-29	38	1AB
2003-09-25	2003-11-19	55	2A
2004-02-17	2004-03-21	34	2B
2004-05-18	2004-06-21	35	2C
2004-10-03	2004-11-08	37	3A
2005-02-17	2005-03-24	36	3B
2005-05-20	2005-06-23	35	3C
2005-10-21	2005-11-24	35	3D
2006-02-22	2006-03-28	34	3E
2006-05-24	2006-06-26	33	3F
2006-10-25	2006-11-27	34	3G
2007-03-12	2007-04-14	34	3H
2007-10-02	2007-11-05	37	3I
2008-02-17	2008-03-21	34	3J
2008-10-04	2008-10-19	16	3K
2008-11-25	2008-12-17	23	2D
2009-03-09	2009-04-11	34	2E
2009-09-30	2009-10-11	12	2F

3 ICESAT ATTITUDES

The ICESat/GLAS spacecraft operates in two attitude modes depending on the angular distance between the orbit plane and the Sun (β' angle). As shown in Figure 3, for low-β' periods, such as that immediately following launch, the so-called "airplane-mode" is in use, with the solar panels perpendicular to the orbit plane. When the β' angle exceeds 32 degrees, however a yaw maneuver places the satellite in the "sailboat-mode", with the axis of solar panels now in the orbit plane.

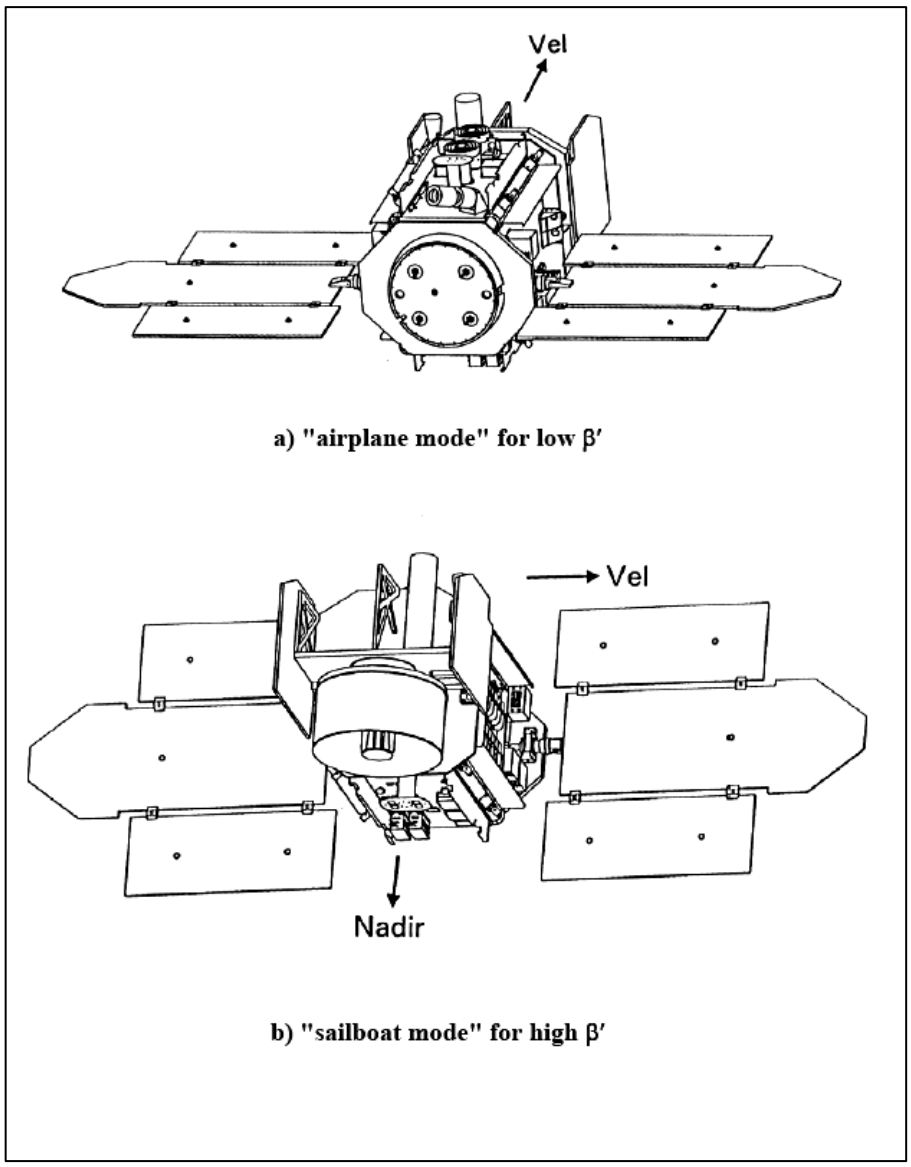

Figure 3. Spacecraft Operation Attitude Modes

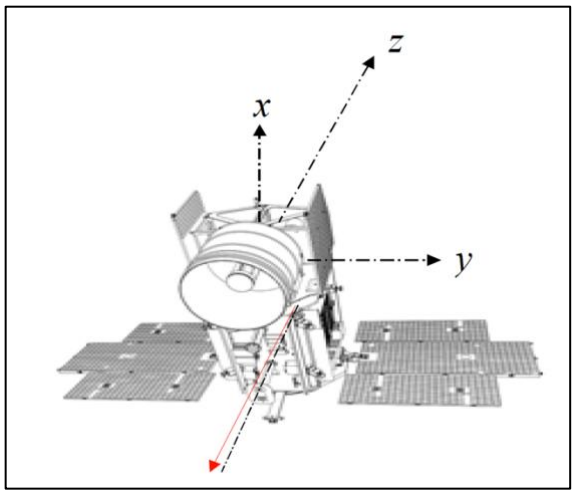

Figure 4. GLAS Coordinate System (GCS) summary. Direction of laser pointing shown in red.

APPENDIX A: NSIDC DISTRIBUTED ICESAT GLAS LASER OPERATIONS PERIODS: LATEST RELEASE

	Notes	Laser 1A Sailboat	Laser 1B Airplane	Laser 2A 8-Day	Laser 2A Pre Delta-T 91-Day	Laser 2A Post Delta-T 91-Day	Laser 2B	Laser 2C	Laser 3A	Laser 3B	Laser 3C	Laser 3D	Laser 3E	Laser 3F	Laser 3G	Laser 3H	Laser 3I	Laser 3J	Laser 3K	Laser 2D	Laser 2E	Laser 2F
Processing Date (month/year)		Jun-14	Jun-14	Jun-14	Jun-14	Jun-14	Jun-14	Jun-14	Jun-14	Jun-14	Jun-14	Jun-14	Jun-14	Jun-14	Jun-14	Jun-14	Jun-14	Jun-14	Jun-14	Jun-14	Jun-14	Jun-14
Start date		2/20/2003	3/21/2003	9/25/2003	10/4/2003	10/13/2003	2/17/2004	5/18/2004	10/3/2004	2/17/2005	5/20/2005	10/21/2005	2/22/2006	5/24/2006	10/25/2006	3/12/2007	10/2/2007	2/17/2008	10/4/2008	11/25/2008	3/9/2009	9/30/2009
End date		3/21/2003	3/29/2003	10/4/2003	10/13/2003	11/19/2003	3/21/2004	6/21/2004	11/8/2004	3/24/2005	6/23/2005	11/24/2005	3/28/2006	6/26/2006	11/27/2006	4/14/2007	11/5/2007	3/21/2008	10/19/2008	12/17/2008	4/11/2009	10/11/2009
Start day of year		51	80	268	277	286	48	139	277	48	140	294	53	144	298	71	275	48	278	330	68	273
End day of year		80	88	277	286	323	81	173	313	83	174	328	87	177	331	104	309	81	293	352	101	284
Orbit Reference ID (RefID)		1102	1102	1102	2103	2103	2107	2107	2109	2111	2111	2113	2115	2115	2117	2119	2121	2123	2125	2127	2129	2131
Duration of repeat orbit cycle (days)		8	8	8	91	91	91	91	91	91	91	91	91	91	91	91	91	91	91	91	91	91
Number of orbit revolutions (tracks) per repeat orbit cycle		119	119	119	1354	1354	1354	1354	1354	1354	1354	1354	1354	1354	1354	1354	1354	1354	1354	1354	1354	1354
Start repeat orbit cycle and track number	1	001 - 72	005 - 25	028 - 88	001 - 1098	001 - 1234	001 - 1284	002 - 1283	001 - 1273	001 - 1258	002 - 1275	001 - 1282	001 - 1283	002 - 1283	001 - 1283	001 - 1279	001 - 1280	001 - 1282	001 - 1283	001 - 96	001 - 1286	001 - 1280
End repeat orbit cycle and track number	1	005 - 24	006 - 23	029 - 100	001 - 1233	002 - 421	002 - 421	003 - 434	002 - 452	002 - 426	003 - 421	002 - 421	002 - 424	003 - 421	002 - 423	002 - 426	002 - 421	002 - 422	002 - 145	001 - 423	002 - 424	002 - 84
Start orbit revolution since launch		580	1009	3809	3941	4077	5972	7314	9383	11421	12792	15090	16936	18290	20581	22630	25681	27737	31159	31936	33483	36542

	Notes	Laser 1A	Laser 1B	Laser 2A	Laser 2A	Laser 2A	Laser 2B	Laser 2C	Laser 3A	Laser 3B	Laser 3C	Laser 3D	Laser 3E	Laser 3F	Laser 3G	Laser 3H	Laser 3I	Laser 3J	Laser 3K	Laser 2D	Laser 2E	Laser 2F
		Sailboat	Airplane	8-Day	Pre Delta-T 91-Day	Post Delta-T 91-Day																
End orbit revolution since launch		1008	1126	3940	4076	4618	6463	7830	9916	11943	13292	15583	17431	18782	21075	23131	26176	28230	31375	32263	33975	36700
Number of repeat orbit cycles completed		3.60	0.98	1.10	0.10	0.40	0.36	0.38	0.39	0.39	0.37	0.36	0.37	0.36	0.36	0.37	0.37	0.36	0.16	0.24	0.36	0.12
Ascending node local time at start and end of operations period (hours:minutes)	2	03:21 - 02:26	02:26 - 02:11	20:27 - 20:10	20:10 - 19:53	19:52 - 18:43	15:49 - 14:46	12:56 - 11:51	08:32 - 07:23	04:10 - 03:03	01:14 - 00:10	20:19 - 19:16	16:22 - 15:19	13:28 - 12:25	08:34 - 07:31	04:11 - 03:07	21:40 - 20:36	17:16 - 16:12	09:57 - 09:30	08:18 - 07:36	04:59 - 03:56	22:26 - 22:06
Latitude range (deg) for near geodetic-nadir pointing (within ~+-2000 meters) (asc)		86S - 86N	86S - 86N	61.3S - 59.1N	61.3S - 59.1N	61.3S - 59.1N	61.3S - 59.1N	61.3S - 59.1N	61.3S - 59.1N	61.3S - 59.1N	61.3S - 46.1N	61.3S - 46.1N	61.3S - 46.1N	61.3S - 46.1N	61.3S - 46.1N	61.3S - 46.1N	61.3S - 46.1N	61.3S - 46.1N	61.3S - 46.1N	61.3S - 46.1N	61.3S - 46.1N	61.3S - 46.1N
Latitude range (deg) for near geodetic-nadir pointing (within ~+-2000 meters) (desc)		86S - 86N	86S - 86N	59.1S - 61.0N	59.1S - 61.0N	59.1S - 61.0N	59.1S - 61.0N	59.1S - 61.0N	59.1S - 61.0N	59.1S - 61.0N	59.1S - 51.8N	59.1S - 51.8N	59.1S - 51.8N	59.1S - 51.8N	59.1S - 51.8N	59.1S - 51.8N	59.1S - 51.8N	59.1S - 51.8N	59.1S - 51.8N	59.1S - 51.8N	59.1S - 51.8N	59.1S - 51.8N
Latitude range (deg) for reference-track pointing (within ~+-100 meters) (asc)		NA	NA	> 61.3S, > 59.1N	> 61.3S, > 59.1N	> 61.3S, > 59.1N	> 61.3S, > 59.1N	> 61.3S, > 59.1N	> 61.3S, > 59.1N	> 61.3S, > 59.1N	> 61.3S, > 46.1N	> 61.3S, > 46.1N	> 61.3S, > 46.1N	> 61.3S, > 46.1N	> 61.3S, > 46.1N	> 61.3S, > 46.1N	> 61.3S, > 46.1N	> 61.3S, > 46.1N	> 61.3S, > 46.1N	> 61.3S, > 46.1N	> 61.3S, > 46.1N	> 61.3S, > 46.1N
Latitude range (deg) for reference-track pointing (within ~+-100 meters) (desc)		NA	NA	> 59.1S, > 61.0N	> 59.1S, > 61.0N	> 59.1S, > 61.0N	> 59.1S, > 61.0N	> 59.1S, > 61.0N	> 59.1S, > 61.0N	> 59.1S, > 61.0N	> 59.1S, > 51.8N	> 59.1S, > 51.8N	> 59.1S, > 51.8N	> 59.1S, > 51.8N	> 59.1S, > 51.8N	> 59.1S, > 51.8N	> 59.1S, > 51.8N	> 59.1S, > 51.8N	> 59.1S, > 51.8N	> 59.1S, > 51.8N	> 59.1S, > 51.8N	> 59.1S, > 51.8N

	Notes	Laser 1A	Laser 1B	Laser 2A	Laser 2A	Laser 2A	Laser 2B	Laser 2C	Laser 3A	Laser 3B	Laser 3C	Laser 3D	Laser 3E	Laser 3F	Laser 3G	Laser 3H	Laser 3I	Laser 3J	Laser 3K	Laser 2D	Laser 2E	Laser 2F
		Sailboat	Airplane	8-Day	Pre Delta-T 91-Day	Post Delta-T 91-Day																
Green (532 nm) laser pulse maximum to minimum transmit energy (mJ)		28 to 20	28 to 20	21 to 14	21 to 14	21 to 14	14 to 0	4 to 0	5 to 5	5 to 3	3 to 2	2 to 2	2 to 1.4	1.6 to 1.4	1.6 to 1	1 to 1	1 to 1	1 to 0.8	0.8 to 0.5	0.9 to 0.5	0.5 to 0	0.4 to 0.3
Green receiver channel (on or off)		off	off	on	on	on	on	on	on	on	on	on	on	on	on	on	on	on	on	on	on	on
Near-infrared (NIR, 1064 nm) laser pulse maximum to minimum transmit energy (mJ)		72 to 51	72 to 51	80 to 55	80 to 55	80 to 55	57 to 33	33 to 5	67 to 62	68 to 54	49 to 44	43 to 39	39 to 30	33 to 30	31 to 24	24 to 22	22 to 20	21 to 16	17 to 12	8 to 4.5	6 to 2	4 to 2.5
Near-infrared elliptical footprint major axis mean and st. dev. (m)	3	148.60 +-9.77	148.60 +-9.77	99.93+ -8.65	99.93+- 8.65	99.93+- 8.65	89.52+ -4.93	88.37+ -19.12	55.79+ -0.43	79.53+ -11.55	55.41+ -1.84	52.04+- 1.06	52.31+ -1.60	51.20+ -1.63	53.41+- 1.51	55.61+ -0.48	57.28+ -0.57	58.66+ -1.52	51.99+- 1.12	NA	NA	NA
Near-infrared elliptical footprint eccentricity mean and st. dev.	3	0.920 +- 0.017	0.920 +- 0.017	0.881+ -0.010	0.881+- 0.010	0.881+- 0.010	0.822+ -0.045	0.892+ -0.044	0.567+ -0.043	0.753+ -0.051	0.633+ -0.034	0.523+- 0.010	0.483+ -0.040	0.480+ -0.023	0.510+- 0.037	0.521+ -0.019	0.590+ -0.013	0.575+ -0.036	0.611+- 0.036	NA	NA	NA
Transmit pulse to receiver field-of-view misalignment (arc sec)	4	NA	NA	~ 36 / 18	~ 36 / 18	~ 36 / 18	~ 36 / 26	NA	NA	NA	NA	NA	NA	NA	NA	NA	NA	NA	NA	NA	NA	NA
Mean and st. dev. of receive-to-transmit pulse NIR energy ratio for region South of -80 degs lat (x e-12)	4	0.286+ -0.037	0.275+ -0.072	0.176+ -0.038	0.176+- 0.033	0.268+- 0.043	0.24+- 0.023	0.292+ -0.074	0.316+ -0.075	0.300+ -0.102	0.265+ -0.043	0.314+- 0.041	0.282+ -0.030	0.271+ -0.032	0.307+- 0.028	0.301+ -0.023	0.312+ -0.031	0.301+ -0.026	0.316+- 0.026	0.215+- 0.046	0.163+ -0.051	0.164+- 0.052
Mean and st. dev. of receive-to-transmit pulse NIR energy ratio for ocean passes (x e-12)	4	0.120+ -0.001	0.122+ -0.001	0.121+ -0.001	0.124+- 0.006	0.121+- 0.001	0.105+ -0.036	0.109+ -0.060	0.123+ -0.001	0.123+ -0.001	0.123+ -0.001	0.124+- 0.001	0.030+ -0.038	0.010+ -0.000	0.025+- 0.037	0.148+ -0.004	0.149+ -0.000	0.149+ -0.000	0.148+- 0.000	0.148+- 0.000	0.149+ -0.000	0.148+- 0.000

	Notes	Laser 1A Sailboat	Laser 1B Airplane	Laser 2A 8-Day	Laser 2A Pre Delta-T 91-Day	Laser 2A Post Delta-T 91-Day	Laser 2B	Laser 2C	Laser 3A	Laser 3B	Laser 3C	Laser 3D	Laser 3E	Laser 3F	Laser 3G	Laser 3H	Laser 3I	Laser 3J	Laser 3K	Laser 2D	Laser 2E	Laser 2F
Ice sheet waveform peak amplitudes that are weak, nominal, and saturated (%)	5	4,83,13	6,85,10	11,88,1	9,90,1	6,89,2	8,88,4	13,86,2	5,82,13	7,88,5	10,86,4	7,89,3	10,86,3	11,85,3	5,92,3	11,87,2	8,90,2	14,85,2	8,90,2	4,95,1	18,82,0	15,85,0
Sea ice waveform peak amplitudes that are weak, nominal, and saturated (%)	5	20,74,6	18,78,4	39,59,2	39,60,2	38,60,2	35,62,3	42,56,2	31,65,5	34,62,4	30,63,6	39,58,3	35,62,3	35,60,4	39,58,3	39,59,2	45,54,2	40,58,1	43,55,2	37,62,1	46,53,0	59,40,1
Land waveform peak amplitudes that are weak, nominal, and saturated (%)	5	11,70,19	10,76,14	22,71,7	23,70,7	24,70,7	16,71,13	23,71,6	20,64,16	15,69,16	19,65,16	22,64,14	17,70,13	19,67,14	23,66,11	17,74,9	22,70,8	20,72,8	21,71,8	29,69,2	27,72,1	27,70,3
Ocean waveform peak amplitudes that are weak, nominal, and saturated (%)	5	15,76,9	15,80,6	33,65,2	32,66,2	34,65,2	26,72,3	34,65,1	30,64,6	27,67,6	26,69,5	30,66,4	28,69,3	27,70,3	28,70,2	29,70,1	28,71,1	34,65,1	26,73,1	37,63,0	49,51,0	40,60,0
Ice sheet waveform saturation duration (nanosecond)	6	9.6	8.8	6.5	6.2	4.4	3.2	3.1	0.7	2.9	3.2	3.2	2.8	2.8	2.7	3.4	3.6	3.2	3.6	1.7	1.7	1.4
Sea ice waveform saturation duration (nanosecond)	6	4.5	3.8	4.4	4.2	4.0	1.8	2.1	2.5	2.6	2.9	1.8	1.3	2.6	1.8	1.7	1.7	1.4	1.8	1.5	1.7	1.4
Land waveform saturation duration (nanosecond)	6	8.4	6.7	6.6	6.6	6.4	4.4	3.4	5.0	4.6	5.2	4.4	3.6	4.6	3.9	3.6	3.7	3.6	3.6	1.9	1.8	3.1
Ocean waveform saturation duration (nanosecond)	6	4.6	4.6	4.6	4.6	4.2	2.7	2.1	2.8	2.8	2.9	2.6	2.4	2.7	2.5	1.8	1.7	1.7	2.0	1.7	1.9	2.2

	Notes	Laser 1A	Laser 1B	Laser 2A	Laser 2A	Laser 2A	Laser 2B	Laser 2C	Laser 3A	Laser 3B	Laser 3C	Laser 3D	Laser 3E	Laser 3F	Laser 3G	Laser 3H	Laser 3I	Laser 3J	Laser 3K	Laser 2D	Laser 2E	Laser 2F
		Sailboat	Airplane	8-Day	Pre Delta-T 91-Day	Post Delta-T 91-Day																
Ice sheet waveform vertical extent (m)	7	81.6	81.6	81.6	81.6	81.6	81.6	81.6	81.6	81.6	81.6	150	150	150	150	150	150	150	150	150	150	150
Land waveform vertical extent (m)	7	81.6	81.6	81.6	81.6	81.6	150	150	150	150	150	150	150	150	150	150	150	150	150	150	150	150
Ocean and sea ice waveform vertical extent (m)	7	30	30	30	30	30	30	30	30	30	30	30	30	30	30	30	30	30	30	30	30	30
S/C orientation (solar arrays w.r.t. velocity vector: airplane = perpendicular, sailboat = parallel)		sailboat	airplane	sailboat	sailboat	sailboat	sailboat	airplane	sailboat	sailboat	airplane	sailboat	sailboat	airplane	sailboat	sailboat	sailboat	sailboat	airplane	sailboat	sailboat	airplane
GLAS coordinate axis in direction of spacecraft velocity vector		-Y	X	Y	Y	Y	Y	-X	-Y	-Y	X	Y	Y	-X	-Y	-Y	Y	Y	X	-Y	-Y	-X
Latest release # and GSAS version for level 1A products (GLA01-4)		R33, V6.0	R33, V6.0	R33, V6.0	R33, V6.0	R33, V6.0	R33, V6.0	R33, V6.0	R33, V6.0	R33, V6.0	R33, V6.0	R33, V6.0	R33, V6.0	R33, V6.0	R33, V6.0	R33, V6.0	R33, V6.0	R33, V6.0	R33, V6.0	R33, V6.0	R33, V6.0	R33, V6.0
Latest release # and GSAS version for atmosphere products (GLA07-11)		R633, V6.0	R633, V6.0	R633, V6.0	R633, V6.0	R633, V6.0	R633, V6.0	R633, V6.0	R633, V6.0	R633, V6.0	R633, V6.0	R633, V6.0	R633, V6.0	R633, V6.0	R633, V6.0	R633, V6.0	R633, V6.0	R633, V6.0	R633, V6.0	R633, V6.0	R633, V6.0	R633, V6.0
Latest release # and GSAS version for altimetry waveform products (GLA05)		R634, V6.1	R634, V6.1	R634, V6.1	R634, V6.1	R634, V6.1	R634, V6.1	R634, V6.1	R634, V6.1	R634, V6.1	R634, V6.1	R634, V6.1	R634, V6.1	R634, V6.1	R634, V6.1	R634, V6.1	R634, V6.1	R634, V6.1	R634, V6.1	R634, V6.1	R634, V6.1	R634, V6.1
Latest release # and GSAS version for altimetry geolocation products (GLA06, GLA12-15)		R634, V6.1	R634, V6.1	R634, V6.1	R634, V6.1	R634, V6.1	R634, V6.1	R634, V6.1	R634, V6.1	R634, V6.1	R634, V6.1	R634, V6.1	R634, V6.1	R634, V6.1	R634, V6.1	R634, V6.1	R634, V6.1	R634, V6.1	R634, V6.1	R634, V6.1	R634, V6.1	R634, V6.1

	Notes	Laser 1A	Laser 1B	Laser 2A	Laser 2A	Laser 2A	Laser 2B	Laser 2C	Laser 3A	Laser 3B	Laser 3C	Laser 3D	Laser 3E	Laser 3F	Laser 3G	Laser 3H	Laser 3I	Laser 3J	Laser 3K	Laser 2D	Laser 2E	Laser 2F
		Sailboat	Airplane	8-Day	Pre Delta-T 91-Day	Post Delta-T 91-Day																
POD SLR residuals (cm): all/ high/radial	8	1.4/NA/ 0.8	1.9 / NA	1.8/1.8/ 1.1	1.8/1.8/ 1.1	1.8/1.8/ 1.1	1.7/NA/ 0.9	2.6/1.1/ 1.7	1.5/NA/ 0.9	1.8/1.6/ 1.0	1.9/1.4/ 1.2	2.1/1.6/ 1.2	1.8/1.8/ 1.1	2.2/1.8/ 1.4	2.6/2.5/ 1.6	1.8/1.8/ 1.2	2.0/1.5/ 1.2	1.8/1.5/ 1.1	1.8/1.5/ 1.1	1.8/1.5/ 1.1	1.8/1.5/ 1.1	1.8/1.5/ 1.1
Calibrations applied to latest geolocation release	9	LRS, ISTD, SM	LRS, ISTD, SM	LRS, ISTD, SM	LRS, ISTD, SM	LRS, ISTD, SM	LRS, ISTD, SM	LRS, ISTD, SM, ISTT, BM	LRS, ISTD, SM	LRS, ISTD, SM	LRS, ISTD, SM, ISTT, BM	LRS, ISTD, SM	LRS, ISTD, SM	LRS, ISTD, SM, ISTT, BM	LRS, ISTD, SM	LRS, ISTD, SM	LRS, ISTD, SM	LRS, ISTD, SM	LRS, ISTD, SM	LRS, ISTD, SM	LRS, ISTD, SM	LRS, ISTD, SM, ISTT, BM
Pointing knowledge accuracy mean and st. dev. (total angle arc sec) for latest geolocation release	10	0.27 +- 1.64	TBD	0.11 +- 1.45	0.11 +- 1.45	0.11 +- 1.45	0.32 +- 1.28	0.13 +- 3.54	0.19 +- 1.13	0.02 +- 1.44	0.10 +- 1.00	0.02 +- 0.98	0.00 +- 1.17	0.47 +- 1.52	0.02 +- 1.16	0.00 +- 1.48	0.22 +- 0.76	0.21 +- 1.60	0.05 +- 1.29	0.59 +- 2.53	0.80 +- 2.75	1.59 +- 5.38
Horizontal geolocation accuracy mean and st. dev. (m)	10	0.79 +- 4.77	TBD	0.33 +- 4.21	0.33 +- 4.21	0.33 +- 4.21	0.93 +- 3.73	0.37 +- 10.30	0.56 +- 3.29	0.07 +- 4.20	0.29 +- 2.92	0.07 +- 2.86	0.00 +- 3.41	1.35 +- 4.42	0.07 +- 3.37	0.00 +- 4.29	0.65 +- 2.22	0.62 +- 4.66	0.15 +- 3.74	1.72 +- 7.36	2.32 +- 8.01	4.63 +- 15.64
Vertical geolocation accuracy mean and st. dev. (cm) per 0.4 deg incidence angle	10, 11	0.6 +- 3.3	TBD	0.2 +- 2.94	0.2 +- 2.94	0.2 +- 2.94	0.7 +- 2.6	0.3 +- 7.2	0.4 +- 2.3	0.1 +- 2.93	0.2 +- 2.04	0.1 +- 2.0	0.0 +- 2.38	1.0 +- 3.08	0.1 +- 2.35	0.0 +- 3.0	0.5 +- 1.55	0.4 +- 3.25	0.1 +- 2.61	1.2 +- 5.14	1.6 +- 5.59	3.2 +- 10.92

Table Notes

NA = not available

TBD = to be determined

1) Repeat orbit cycle refers to each distinct orbit geometry, designated by the Orbit RefID, and is numbered consecutively beginning with 001. A cycle consists of 119 orbit tracks for the 8-day orbit period, or 1354 orbit tracks for the 91-day orbit period. Distinct orbit geometries are separated by spacecraft maneuvers, such as changing between the 8-day and 91-day orbit periods.

2) Approximate local time at which the spacecraft crosses the equator on the ascending portion of an orbit. The local time of the descending crossing of the equator occurs approximately 12 hours later. These times can be used to determine the illumination conditions (daytime or nighttime) during data acquisition. ICESat is in a 96-degree inclination, retrograde orbit so ascending tracks cross the equator from SSE to NNW and descending tracks cross from NNE to SSW.

3) Mean and standard deviation of elliptical footprint major axis length and eccentricity computed where energy has decreased to 1/e^2 of the peak (13.5%), determined from all LPA laser spot far-field images.

4) Misalignment magnitude from green-channel LBSM field-of-view (FOV) scans. LBSM scans are not available when the green receiver channel is off (Laser 1) or green transmit energy is low. The two values for L2a and L2b are the misalignment and energy ratios before and after instrument temperature anomalies, occurring on DOY 286 and 50, respectively. Large misalignment (e.g., first part of L2a and early in L2b) causes FOV shadowing that lowers the receive-to-transmit energy ratio, and skews NIR received waveform shape when the incidence angle between laser vector and surface normal is not zero. Prior to Release 24, errors in transmit and receive energy computations made the energy ratio results inconsistent. Correct energy ratios will be computed as Release 24 (or later) becomes available for each operations period.

Antarctic energy ratios are computed by taking the campaign average of the ratios of the received to transmitted energies averaged over each track, using only shots for which the gain was below a threshold that varied with laser energy (as a way to avoid effects due to clouds) when the spacecraft was south of -80 degs latitude. Ocean energy ratios are computed from the same data subsets as Rows 53-55, i.e., 1-Hz smoothed ocean data are averaged between +-65 degrees and

over waters with depths > 500 m. Statistics are the average and st. dev. of the daily global mean of parameter i_reflctUncorr, excluding partial days.

5) Defined by altimetry channel maximum digitizer count: weak < 35, 35 < nominal < 220, saturated > 220, categorized by acquisition mask surface type. Values are means of daily percentages. Maximum digitizer count depends on transmit energy, atmospheric transmissivity, surface reflectance and relief, transmit pulse to receiver FOV alignment, and receiver gain as adjusted by the automated gain loop. Sea ice values are for the area of its maximum extent and are thus a mixture of open ocean and sea ice that is seasonally dependent. Two sets of values are provided for the L2a 91-day repeat orbit period, corresponding to data before and after the instrument temperature anomaly on DOY 286.

6) Duration that altimetry channel digitizer counts are above 220, for waveforms designated as saturated, categorized by acquisition mask surface type. Values are averages of daily medians. Saturation occurs when the return energy at the detector gain level exceeds the linear response range of the receiver, causing distortion of the waveform (flat-topped and broadened, followed by an abrupt signal decrease and low-amplitude oscillations). Sea ice values are for the area of its maximum extent and are thus a mixture of open ocean and sea ice that is seasonally dependent. Two sets of values are provided for the L2a 91-day repeat orbit period, corresponding to data before and after the instrument temperature anomaly on DOY 286.

7) 81.6 m = 544 gates sampled at 0.15 m per gate. 150 m = gates 1 through 151 sampled at 0.60 m per gate, by 4x averaging, and gates 152 through 544 sampled at 0.15 m per gate. 30 m = 200 gates sampled at 0.15 m per gate. Where the vertical extent of the received signal exceeds the waveform extent, the signal from higher surfaces in the laser footprint is truncated (extends above the first waveform gate) and the reported signal start is positioned at the first gate. When the waveform is truncated, signal start (highest detected surface), signal centroid (alternate elevation), and Gaussian fit (standard elevation) are too low.

8) Satellite Laser Ranging (SLR) data are independent observations of the spacecraft's orbital position. Statistics cited here are RMS values of the SLR range residuals, based on comparisons with the GPS POD solutions. They are computed for each campaign (L1, L2a not split). The first number ("all") is based on all SLR observations during that campaign and is, therefore, representative of the 3-D orbit accuracy. The second number ("high") is based only on SLR observations collected at elevation angles between 60 and 70 degrees ("elevation" here meaning the local angle upward from the horizon at each SLR station), and thus approximates the orbit accuracy in the radial direction. The third number ("radial") is based on a calculation which relates each SLR observation to radial and other components based on the SLR pass geometry, and thus also approximates the orbit accuracy in the radial direction. For some campaigns, the "high"

numbers are not available (NA), due to a lack of observations at the required elevation angles. Note that SLR ranging to ICESat is prohibited at elevations above

Update 3/12/2008: POD comparison statistics for the orbits applied to the final data products (currently Release 428) have been recalculated using the ITRF-2005 reference frame for SLR stations.

9) LRS = Laser Reference System, P-LRS = Pseudo-Laser Reference System (used during Laser 1 and periods of low green transmit energy), ISTD = Instrument Star Tracker Distortion, ATF = Arc-Tangent Fix, SM = ocean and round-the-world 5-degree scan maneuvers, BSTR = BST replacement of IST during sun blinding, ISTT = IST time- tag corrections, BM = Batch Method for sun blinding.

10) These represent accuracies averaged over long wavelengths (~1/4 orbit rev) estimated by Integrated Residual Analysis using calibration scan maneuvers and crossovers. There could be higher frequency geolocation errors not detected by current calibration and validation methods. Incidence angle is the angle between the laser vector and the surface normal. The effect of field-of-view (FOV) shadowing on range residuals is identical to a pointing error, and is thus accounted for in the scan maneuver pointing calibration. Pointing errors and FOV shadowing exhibit temporal correlation on orbital and longer periods and thus the resulting vertical errors are not random, exhibiting spatially correlated errors across a surface where the incidence angle is uniform. These spatially correlated errors can introduce apparent elevation change between ascending and descending orbit tracks and/or between laser operations periods.

11) Vertical accuracy applies to non-saturated, non-cloud returns from planar surfaces that are not affected by atmospheric forward scattering caused by transmission through low, thin clouds. The severity of saturation, causing waveform broadening and a derived elevation that is too low, is a function of received energy and receiver gain and is quantified by the duration of digitizer output above 220 beginning with Release 24. Saturation at the lowest gain (13) occurs when the received energy exceeds the linear response range of the GLAS receiver, typical of clear-atmosphere snow and ice surfaces when NIR transmit energy is high, and specular, smooth water surfaces. Saturation at higher gains occurs for short periods while the automated gain loop adjusts in response to abrupt transitions in peak received energy (due to changes from low to high reflectance, rugged to flat surfaces, and/or cloudy to clear atmosphere).

A laboratory-calibrated range correction, applicable only to low-slope, low-relief surfaces, for saturated returns with gain of 13 is available in GLA06 and GLA12-15 beginning with Release 24, and will be available for all gains beginning with Release 25. Returns from clouds can be identified by waveform character (broad signal extent; low maximum received energy), elevations significantly above the associated DEM value and/or correlation with cloud tops identified in the

atmosphere products. The severity of atmospheric forward scattering, causing broadening of the waveform and a derived elevation that is too low, is a function of cloud optical depth, height, vertical extent, and particle size. The possible presence of atmospheric forward scattering per laser shot is indicated by measures of 1064 nm integrated atmospheric backscatter and cloud height available in GLA06 and GLA12-15 at 40 Hz beginning with Release 24.

A model-based forward scattering range correction estimate of TBD accuracy for the L2a and L2b operation periods based on the 532 nm channel atmospheric products is available in GLA06 and GLA12-15 at 1 Hz beginning with Release 18. A model-based forward scattering range correction for all laser operations periods based on 1064 nm channel atmospheric products may be available in a future release. Waveform saturation and atmospheric forward scattering elevation errors, each of which can be at the cm to m level, can be coupled and offsetting. Increased cloud cover reduces saturation range error but can increase forward scattering range error.

12) ICESat 1-Hz normal points were created for comparison to 1-Hz radar altimetry elevations and a model of Mean Sea Surface (MSS). Ocean data are averaged between +-65 degrees and over waters with depths > 500 m. Table statistics are the average and st. dev. of the daily statistics, excluding partial days (first & last of a campaign). The MSS model used is GSFC00. The GLA15 - MSS ocean bias (Row 53) has been adjusted to remove the seasonal signal, calculated using either TOPEX (from L1a to L3c) or Jason-1 (from L3d onward; with a 15.0 cm relative T/J bias applied) over the similar campaign time span. When radar data lags the most recent campaign, e.g. L3e as of 4/6/2006, Row 53 will be adjusted by an average from similar seasons in past years, until Jason radar altimetry is obtained. As a reference for comparison, Row 53 for TOPEX (Jason) averaged over campaigns L1a-L3c (L1a-L3d) is 13.7 cm (9.0 cm); Row 55 for TOPEX (Jason) averaged over campaigns L1a-L3c (L1a-L3d) is 0.1 +- 2.2 cm (-0.4 +- 1.1 cm).

13) Elevations have had ocean tide and load tide corrections applied using the GOT99.2 global ocean model [Ray,1999]. Ray, R.D. (1999), A global ocean tide model from TOPEX/Poseidon altimetry: GOT99.2, NASA Tech. Memo., 209478, 58 pp. As of release 33, the global ocean model used is TPXO7.1.

14) SRTM 90 m DEM elevation value for pixel in which ICESat footprint latitude/longitude is located. SRTM WGS- 84 orthometric elevations have been converted toTOPEX/Poseidon ellipsoid elevations using EGM-96 geoid and WGS-84 to T/P ellipsoid transformation. JPL SRTM is the so called "unfinished" product which computes the 90 m pixel elevation from the average of 3 x 3 30 m pixel patches. NGA SRTM is the so called "finished" product which is a subsampled elevation which equates the 90 m pixel elevation to the center pixel of 3 x 3 30 m pixel patches. The "finished" product also flattens water and fills small voids by interpolation.

15) Saturation range correction is a function of receiver gain and accounts for pulse broadening due to saturation, based on laboratory calibrations.

16) Forward scattering range correction estimates range delay due to multiple scattering through clouds layers, based on atmospheric channel measurements of cloud optical depth, height, and thickness and a seasonally and latitudinally dependent model of cloud particle size. The particle size model does not capture its true variability and is thus a potential source of significant error in the range delay estimate. Computation of the correction is presently limited to periods when 532 nm channel data with high S/N is available. In the future, an estimate (of less accuracy) may be produced using 1064 nm channel atmospheric data.

References

Special Section: Results from Ice, Cloud, and land Elevation Satellite (ICESat) Mission
GEOPHYSICAL RESEARCH LETTERS, VOL. 32, NO. 21 and 22, 2005
Selected papers on instrumentation, measurement descriptions, and calibration/validation

Abshire, J. B., X. Sun, H. Riris, J. M. Sirota, J. F. McGarry, S. Palm, D. Yi, and P. Liiva (2005), Geoscience Laser Altimeter System (GLAS) on the ICESat Mission: On-orbit measurement performance, Geophys. Res. Lett., 32, L21S02,

Fricker, H. A., A. Borsa, B. Minster, C. Carabajal, K. Quinn, and B. Bills (2005), Assessment of ICESat performance at the salar de Uyuni, Bolivia, Geophys. Res. Lett., 32, L21S06, doi:10.1029/2005GL023423.

Harding, D. J., and C. C. Carabajal (2005), ICESat waveform measurements of within-footprint topographic relief and vegetation vertical structure, Geophys. Res. Lett., 32, L21S10, doi:10.1029/2005GL023471.

Luthcke, S. B., D. D. Rowlands, T. A. Williams, and M. Sirota (2005), Reduction of ICESat systematic geolocation errors and the impact on ice sheet elevation change detection, Geophys. Res. Lett., doi:10.1029/2005GL023689.

Magruder, L., E. Silverberg, C. Webb, and B. Schutz (2005), In situ timing and pointing verification of the ICESat altimeter using a ground-based system, Geophys. Res. Lett., 32, L21S04, doi:10.1029/2005GL023504.

Martin, C. F., R. H. Thomas, W. B. Krabill, and S. S. Manizade (2005), ICESat range and mounting bias estimation over precisely-surveyed terrain, Geophys. Res. Lett., 32, L21S07, doi:10.1029/2005GL023800.

Geophys. Res. Lett., 32, L21S01, doi:10.1029/2005GL024009.

Sirota, J. M., S. Bae, P. Millar, D. Mostofi, C. Webb, B. Schutz, and S. Luthcke (2005), The transmitter pointing determination in the Geoscience Laser Altimeter System, Geophys. Res. Lett., 32, L22S11, doi:10.1029/2005GL024005.

Spinhirne, J. D., S. P. Palm, W. D. Hart, D. L. Hlavka, and E. J. Welton (2005), Cloud and aerosol measurements from GLAS: Overview and initial results, Geophys. Res. Lett., 32, L22S03, doi:10.1029/2005GL023507.

Urban, T. J., and B. E. Schutz (2005), ICESat sea level comparisons, Geophys. Res. Lett., 32, L23S10

APPENDIX B: ICESAT WORLD MAPS 2

ICESat Altimetry Campaigns - 2003-2009 C

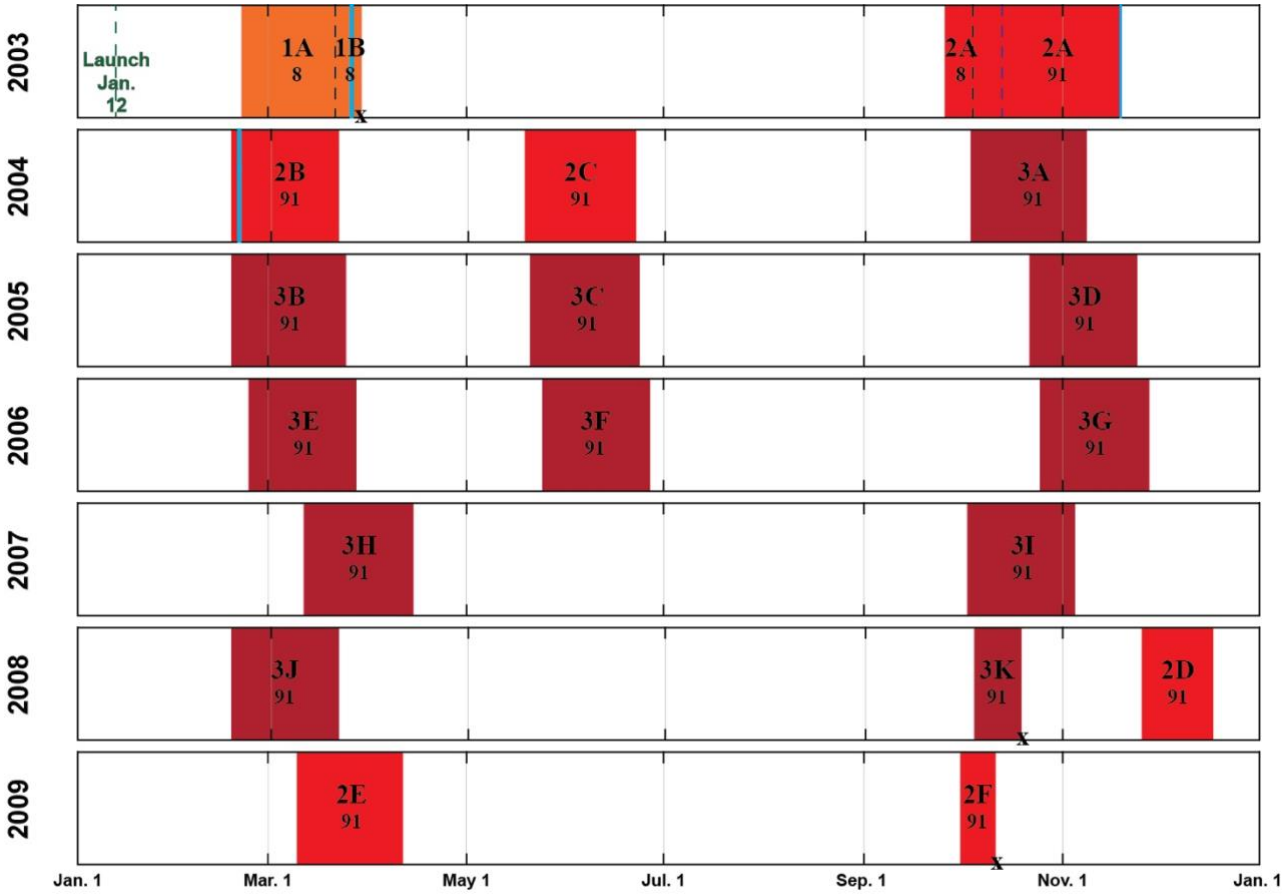

SAM = Sun Acquisition Manuever, no altimetry collected, X's = laser failures, dashed lines indicate on-orbit change in instrument attributes.
Information from: http://icesat.gsfc.nasa.gov/icesat/missionevents.php
and http://nsidc.org/data/icesat/laser_op_periods.html (glas_laser_ops_attrib.xls)

Year	Ops. Period (days)	Start-Stop Dates	Mode	Pattern(s)
2003	1 Laser 1A/B (38)	Feb. 20 - Mar. 29, 2003*	sail./air.	8-day (~5)
	2 Laser 2A (55)	Sep. - Nov. 19, 2003	sailboat	8&91-day
2004	3 Laser 2B (33)	Feb. 17 - Mar. 21, 2004	sailboat	91-day
	4 Laser 2C (35)	May 18 - Jun. 21, 2004	airplane	91-day
	5 Laser 3A (37)	Oct. 3 - Nov. 8, 2004	sailboat	91-day
2005	6 Laser 3B (36)	Feb. 17 - Mar. 24, 2005	sailboat	91-day
	7 Laser 3C (35)	May 20 - Jun. 23, 2005	airplane	91-day
	8 Laser 3D (34)	Oct. 21 - Nov. 24, 2005	sailboat	91-day
2006	9 Laser 3E (34)	Feb. 22 - Mar. 28, 2006	sailboat	91-day
	10 Laser 3F (34)	May 24 - Jun. 26, 2006	airplane	91-day
	11 Laser 3G (34)	Oct. 25 - Nov. 27, 2006	sailboat	91-day
2007	12 Laser 3H (34)	Mar. 12 - Apr. 14, 2007	sailboat	91-day
	13 Laser 3I (34)	Oct. 2 - Nov. 5, 2007	sailboat	91-day
2008	14 Laser 3J (34)	Feb. 17 - Mar. 21, 2008	sailboat	91-day
	15 Laser 3K (15)	Oct. 4 - Oct. 19, 2008*	airplane	91-day
	16 Laser 2D (23)	Nov. 25 - Dec. 17, 2008	sailboat	91-day
2009	17 Laser 2E (34)	Mar. 9 - Apr. 11, 2009	sailboat	91-day
	18 Laser 2F (12)	Sep. 30 - Oct. 11, 2009*	airplane	91-day

'Sailboat' means ICESat was oriented with solar panels parallel to motion vector, 'Airplane' means ICESat was oriented with solar panels perpendicular to motion, 8-day or 91-day (~33-day subcycle) describes time needed to complete a full global pattern (see track maps at NSIDC). Asterisk* means end of laser life, 3 total onboard.

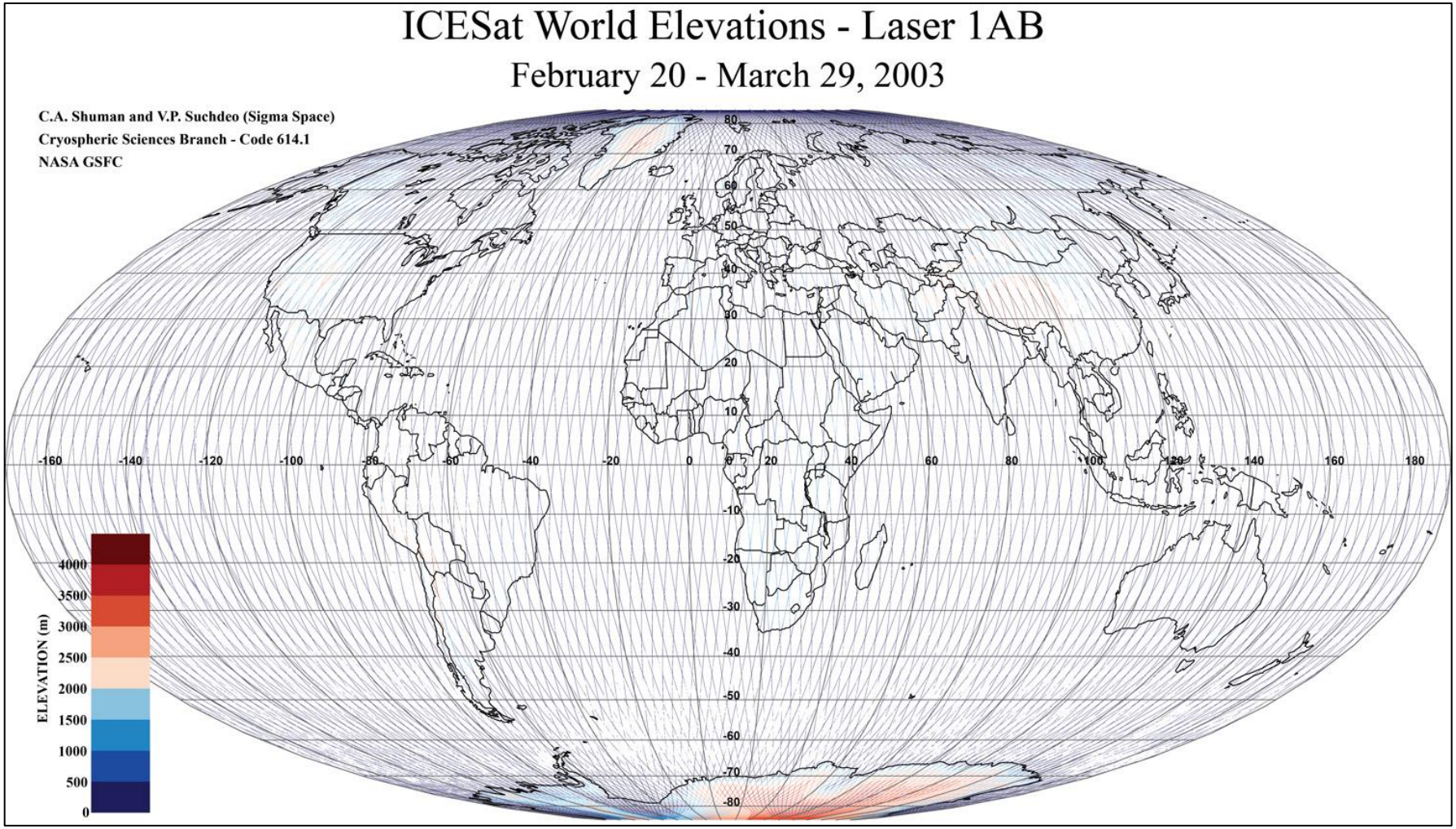
ICESat World Elevations - Laser 1AB
February 20 - March 29, 2003
C.A. Shuman and V.P. Suchdeo (Sigma Space)
Cryospheric Sciences Branch - Code 614.1
NASA GSFC
ELEVATION (m)
4000
3500
3000
2500
2000
1500
1000
500
0
80
70
60
50
40
30
20
10
-10
-20
-30
-40
-50
-60
-70
-80
-160
-140
-120
-100
-80
-60
-40
-20
0
20
40
60
80
100
120
140
160
180

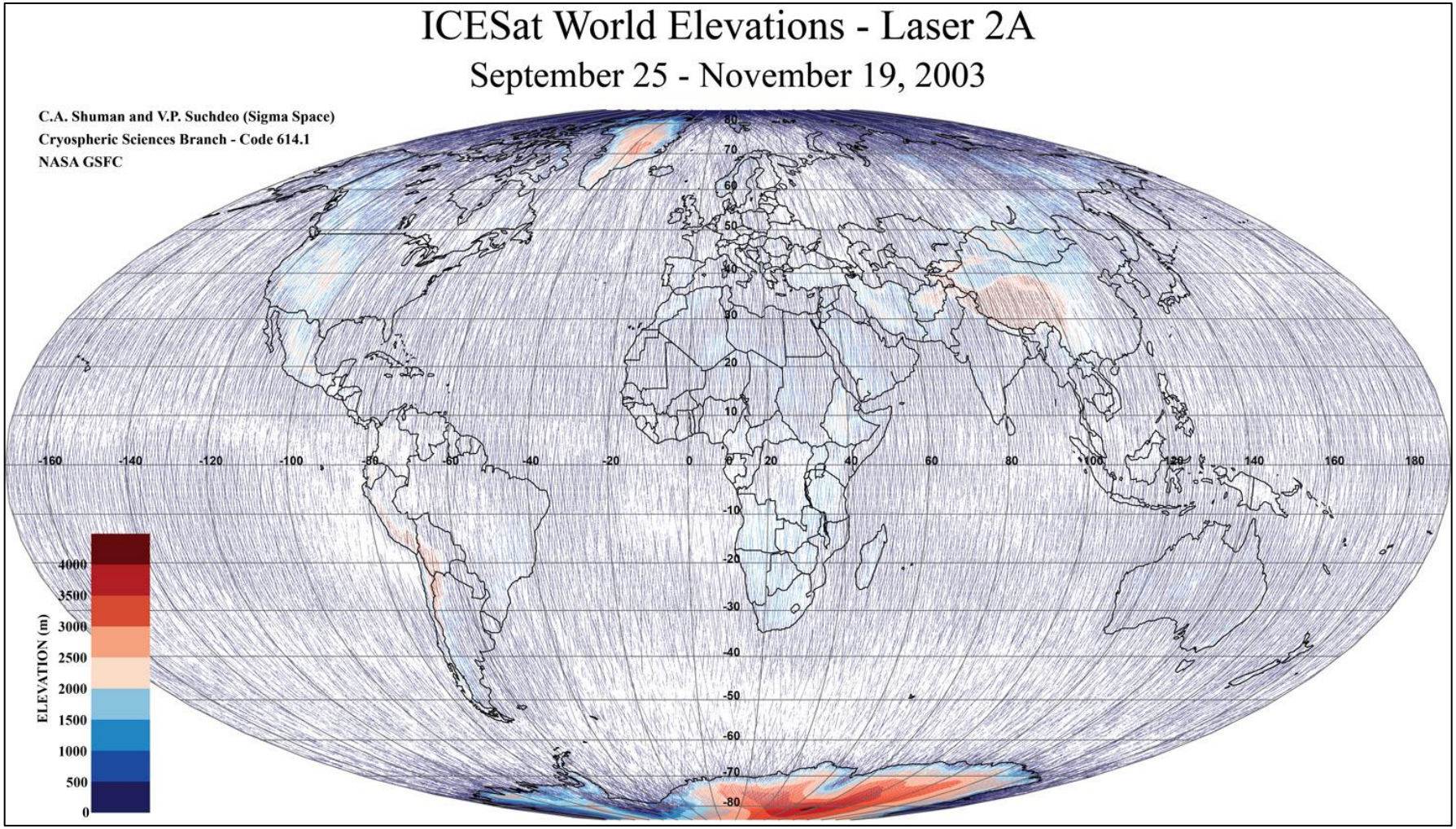
ICESat World Elevations - Laser 2A
September 25 - November 19, 2003
C.A. Shuman and V.P. Suchdeo (Sigma Space)
Cryospheric Sciences Branch - Code 614.1
NASA GSFC
ELEVATION (m)
4000
3500
3000
2500
2000
1500
1000
500
0

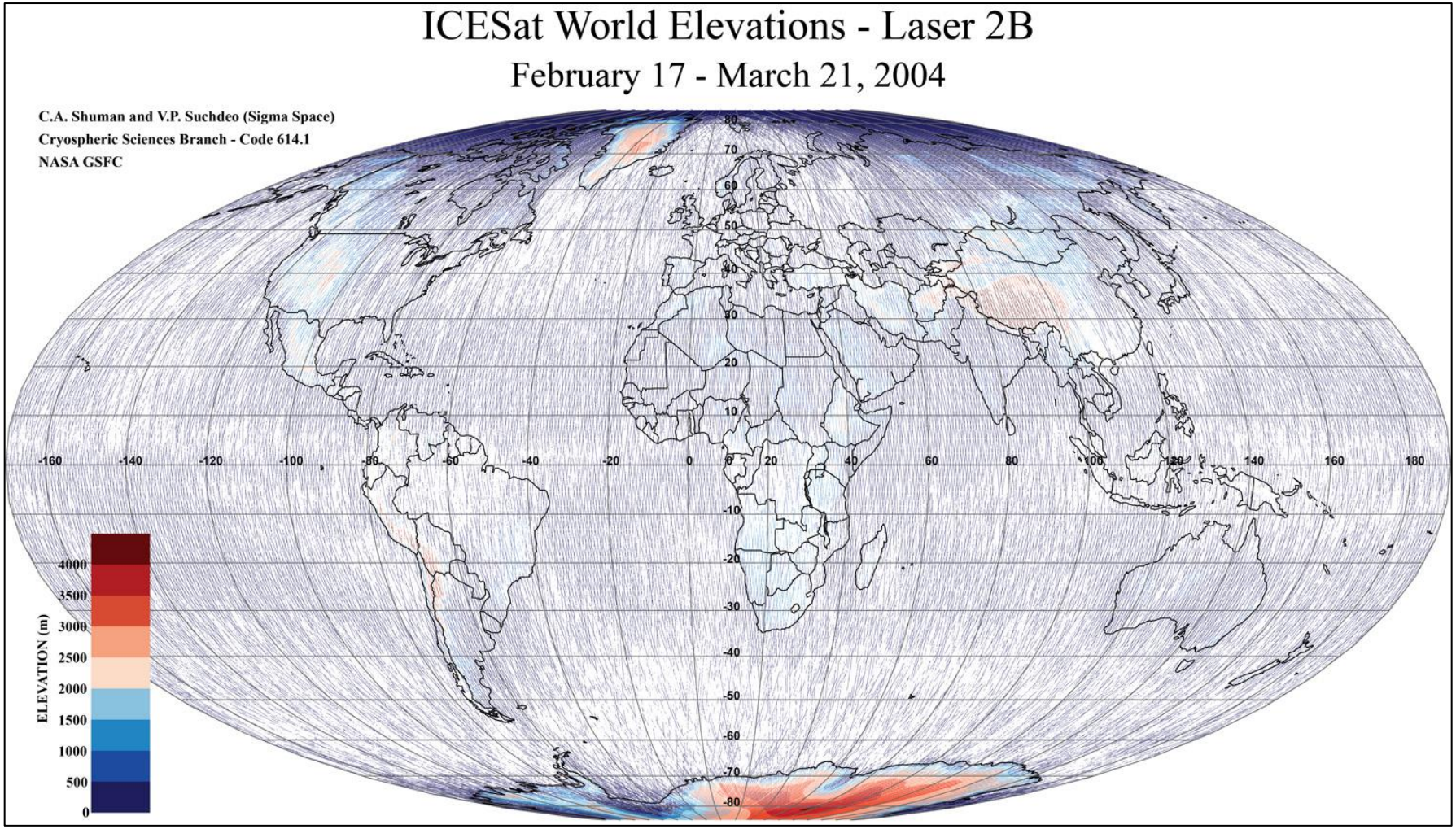
ICESat World Elevations - Laser 2B
February 17 - March 21, 2004
C.A. Shuman and V.P. Suchdeo (Sigma Space)
Cryospheric Sciences Branch - Code 614.1
NASA GSFC
ELEVATION (m)
4000
3500
3000
2500
2000
1500
1000
500
0

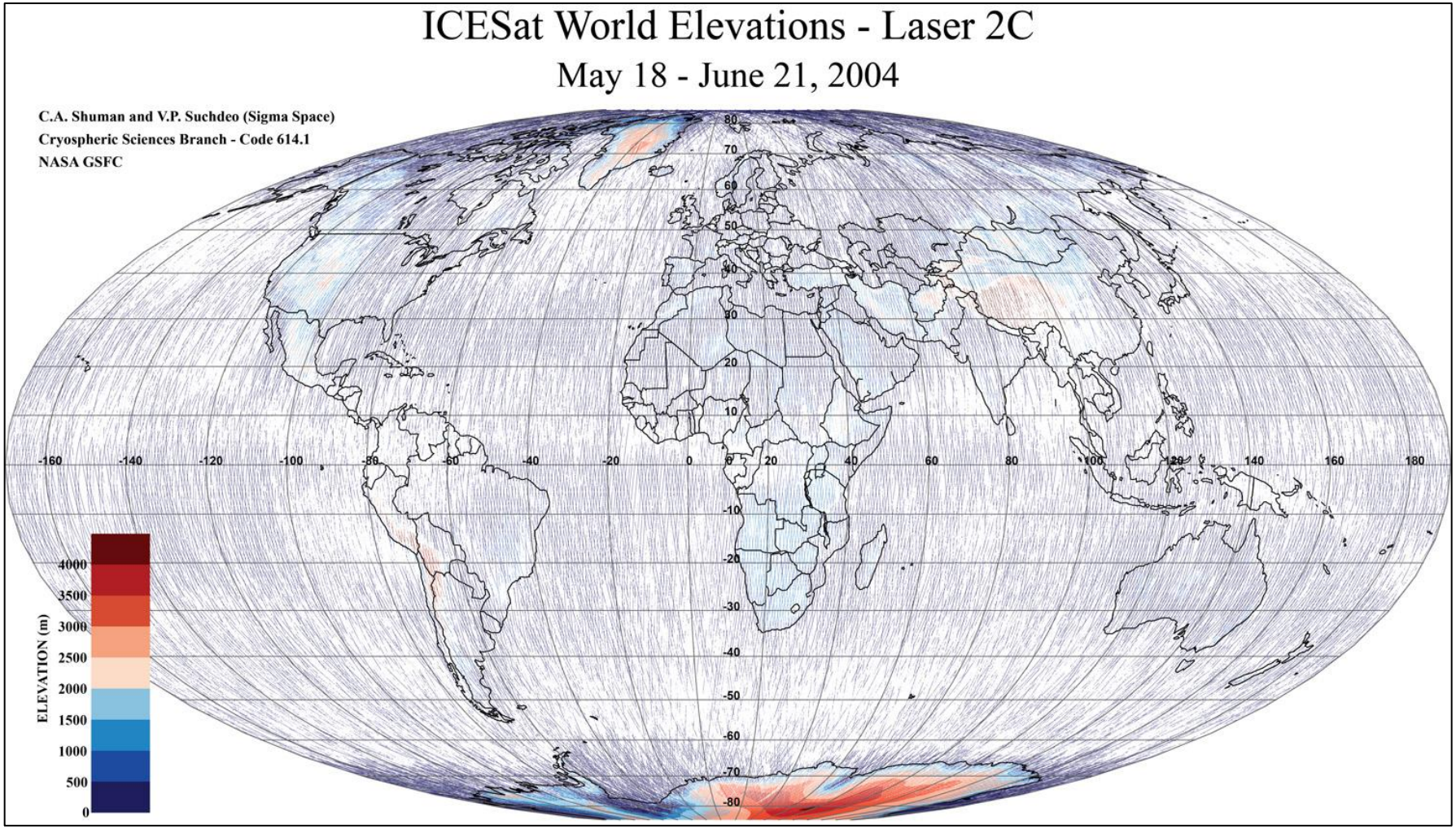
ICESat World Elevations - Laser 2C
May 18 - June 21, 2004
C.A. Shuman and V.P. Suchdeo (Sigma Space)
Cryospheric Sciences Branch - Code 614.1
NASA GSFC
ELEVATION (m)
4000
3500
3000
2500
2000
1500
1000
500
0

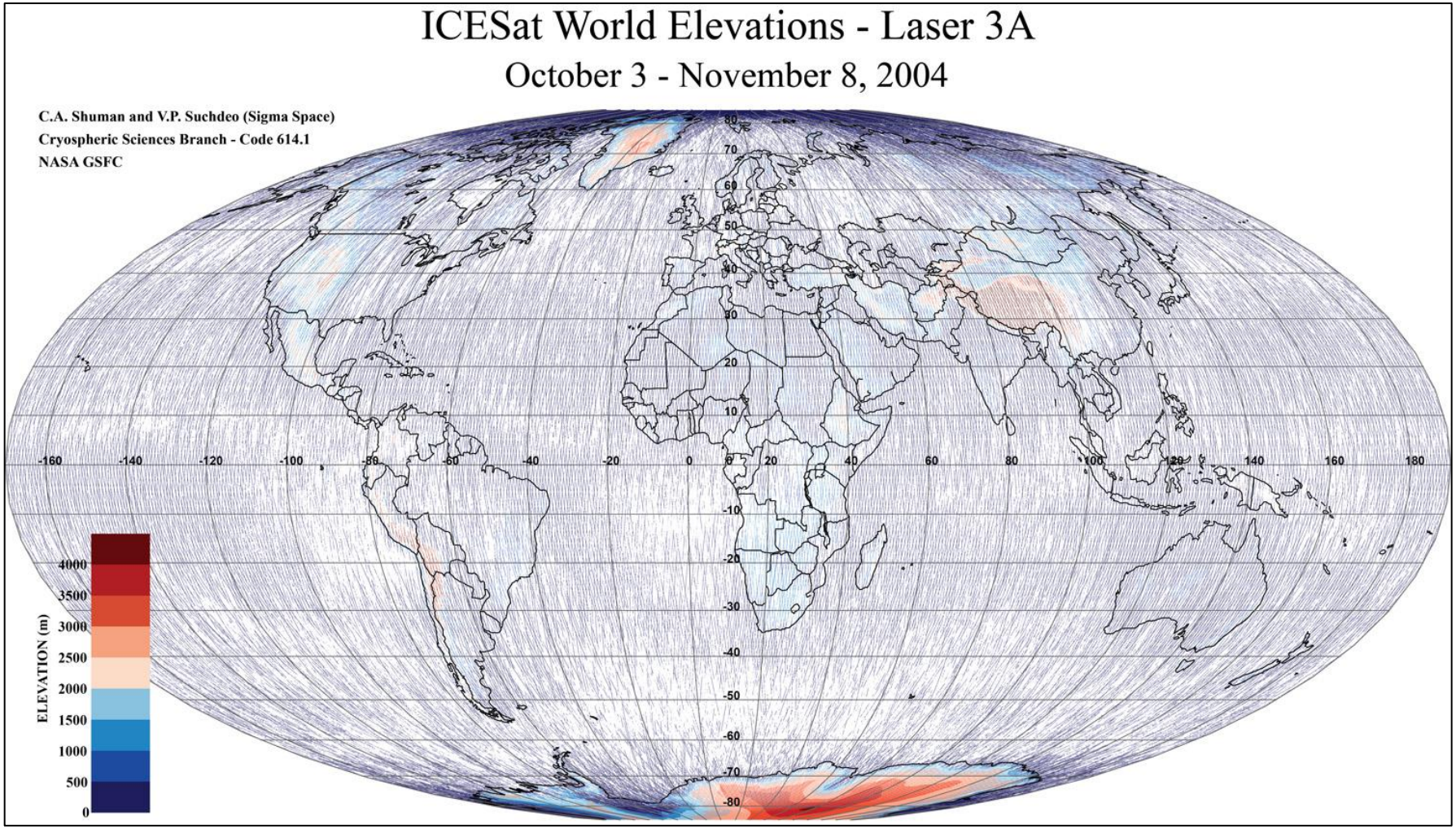
ICESat World Elevations - Laser 3A
October 3 - November 8, 2004
C.A. Shuman and V.P. Suchdeo (Sigma Space)
Cryospheric Sciences Branch - Code 614.1
NASA GSFC
ELEVATION (m)
4000
3500
3000
2500
2000
1500
1000
500
0

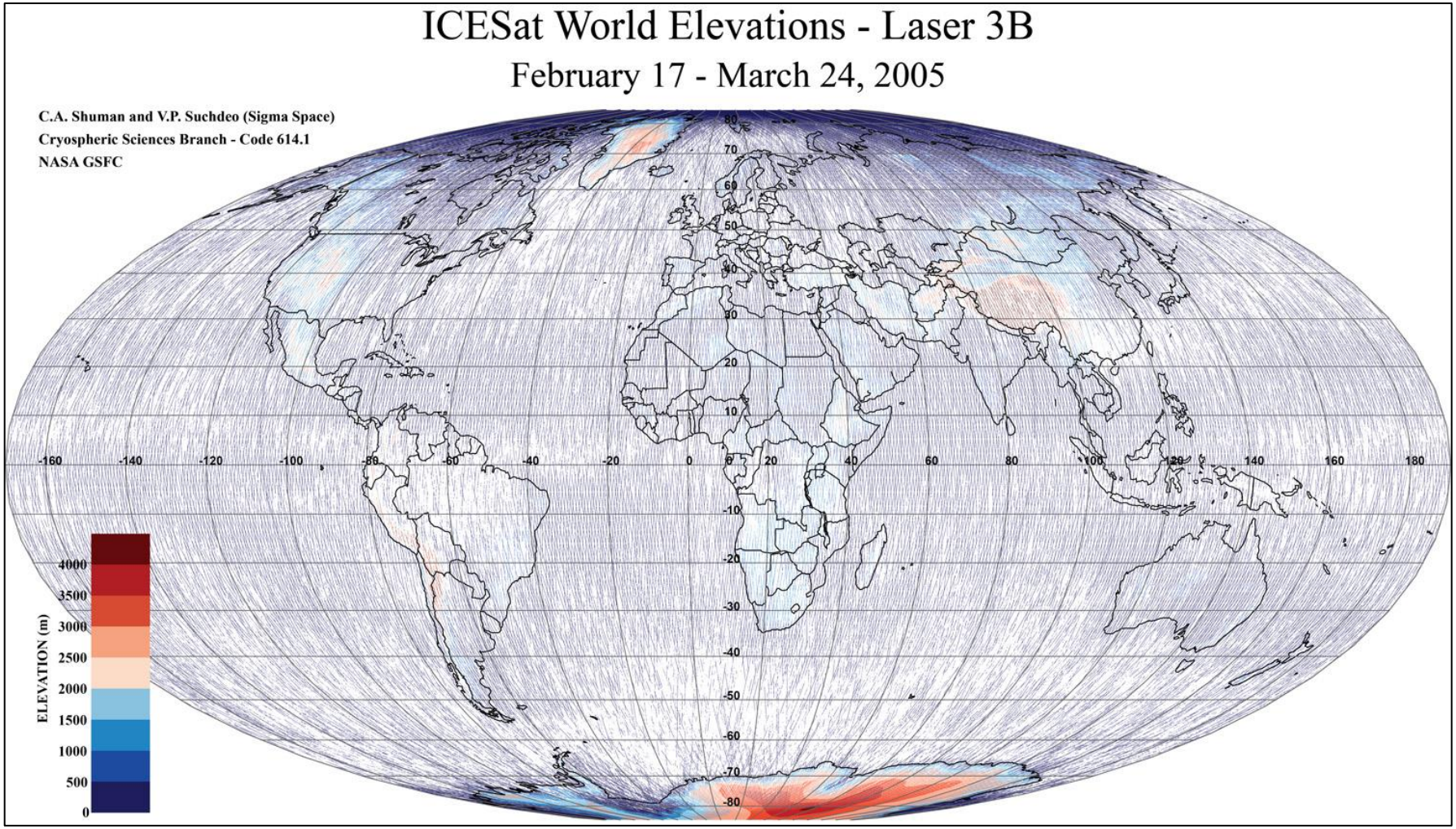
ICESat World Elevations - Laser 3B
February 17 - March 24, 2005
C.A. Shuman and V.P. Suchdeo (Sigma Space)
Cryospheric Sciences Branch - Code 614.1
NASA GSFC
ELEVATION (m)
4000
3500
3000
2500
2000
1500
1000
500
0

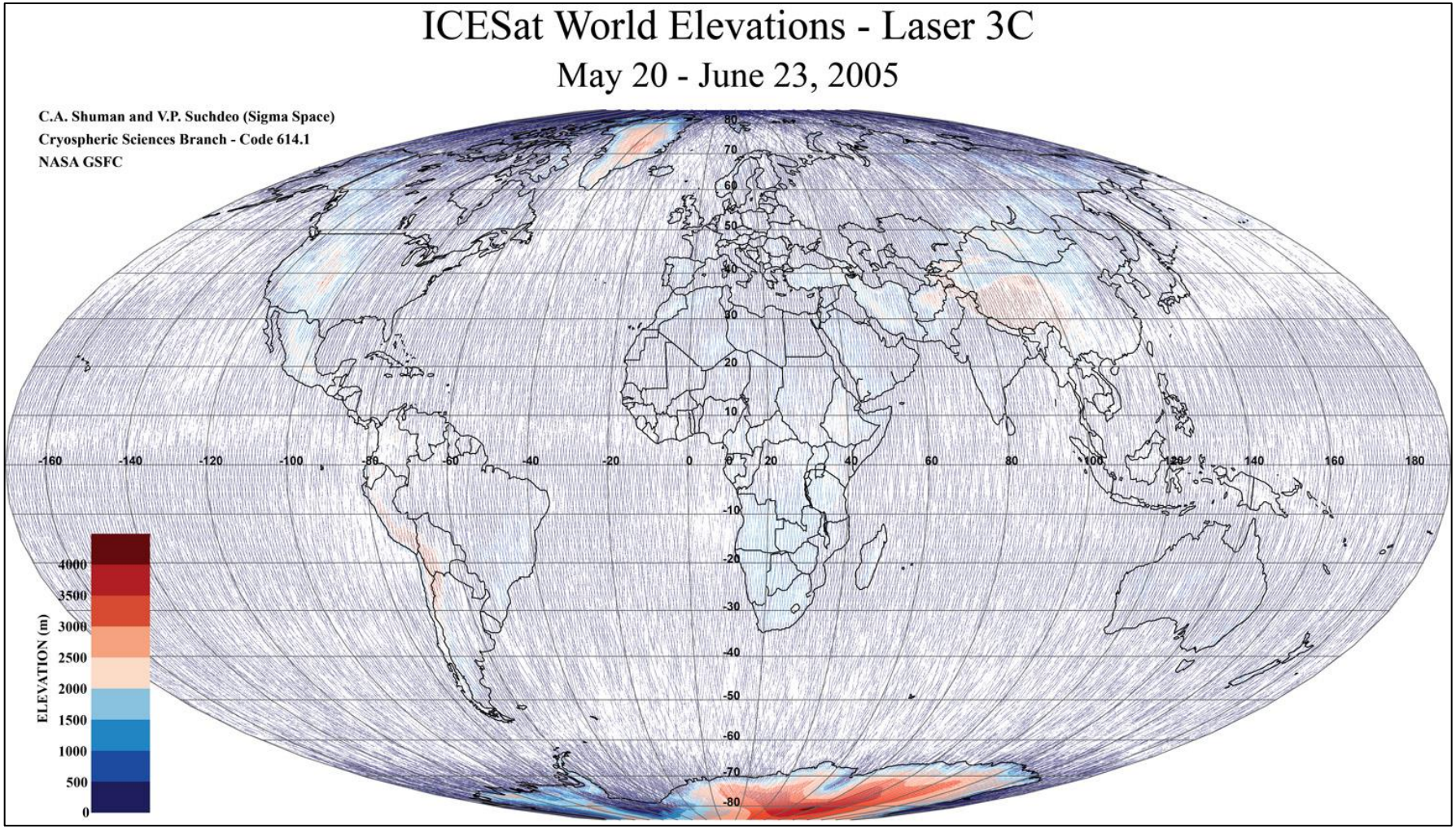
ICESat World Elevations - Laser 3C
May 20 - June 23, 2005
C.A. Shuman and V.P. Suchdeo (Sigma Space)
Cryospheric Sciences Branch - Code 614.1
NASA GSFC
ELEVATION (m)
4000
3500
3000
2500
2000
1500
1000
500
0

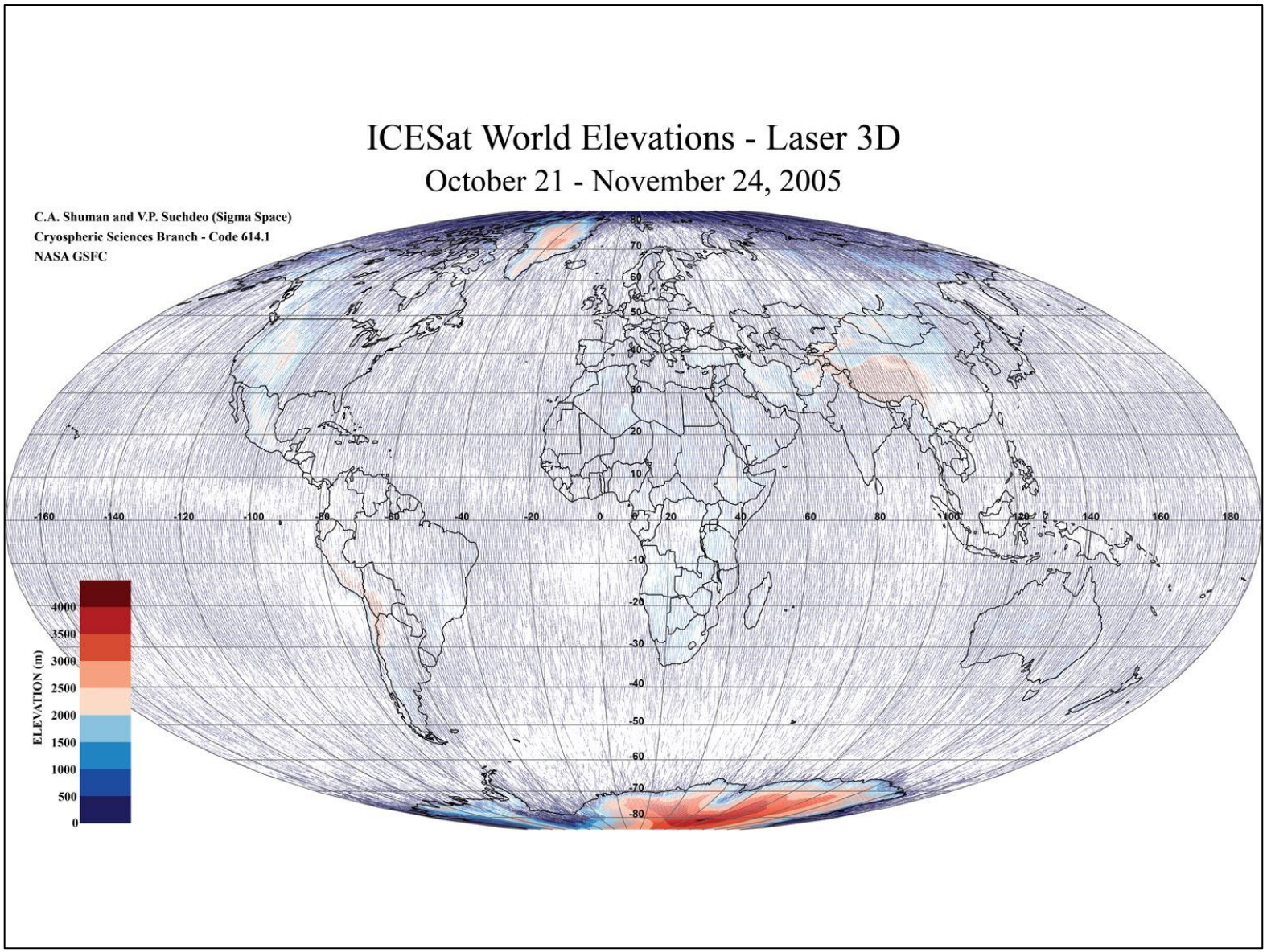
ICESat World Elevations - Laser 3D
October 21 - November 24, 2005
C.A. Shuman and V.P. Suchdeo (Sigma Space)
Cryospheric Sciences Branch - Code 614.1
NASA GSFC
ELEVATION (m)
4000
3500
3000
2500
2000
1500
1000
500
0

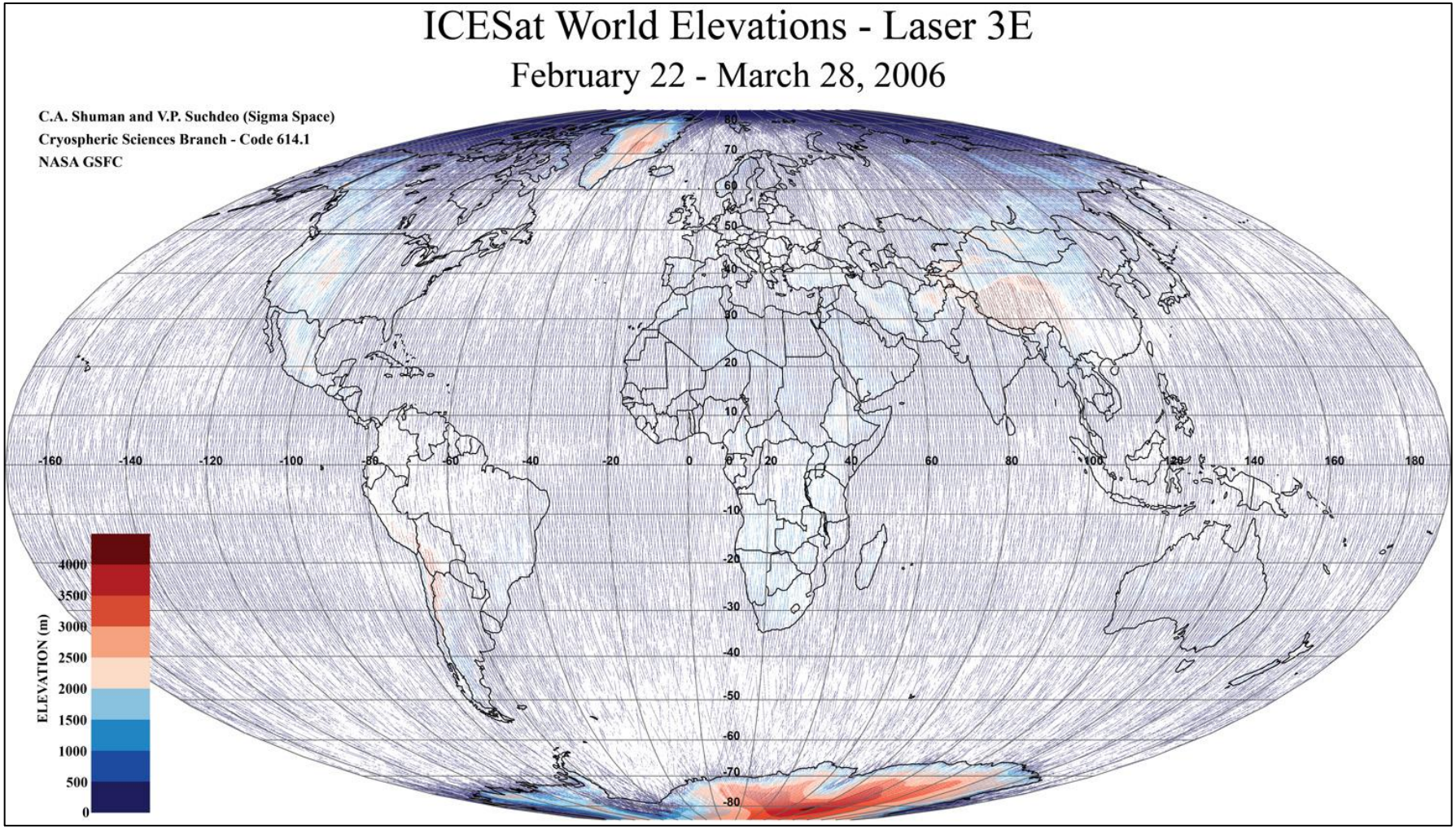
ICESat World Elevations - Laser 3E
February 22 - March 28, 2006
C.A. Shuman and V.P. Suchdeo (Sigma Space)
Cryospheric Sciences Branch - Code 614.1
NASA GSFC
ELEVATION (m)
4000
3500
3000
2500
2000
1500
1000
500
0

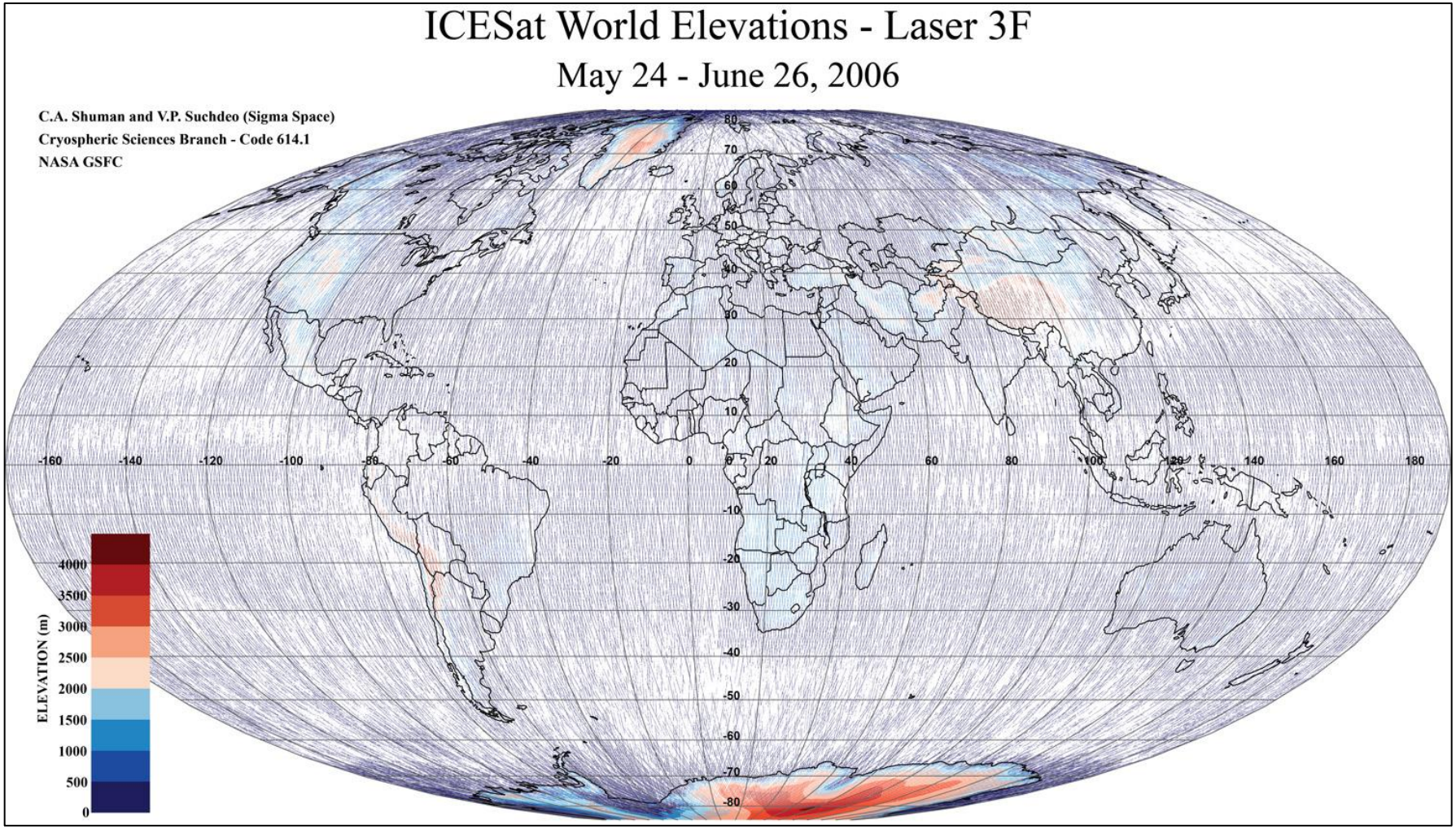
ICESat World Elevations - Laser 3F
May 24 - June 26, 2006
C.A. Shuman and V.P. Suchdeo (Sigma Space)
Cryospheric Sciences Branch - Code 614.1
NASA GSFC
ELEVATION (m)
4000
3500
3000
2500
2000
1500
1000
500
0

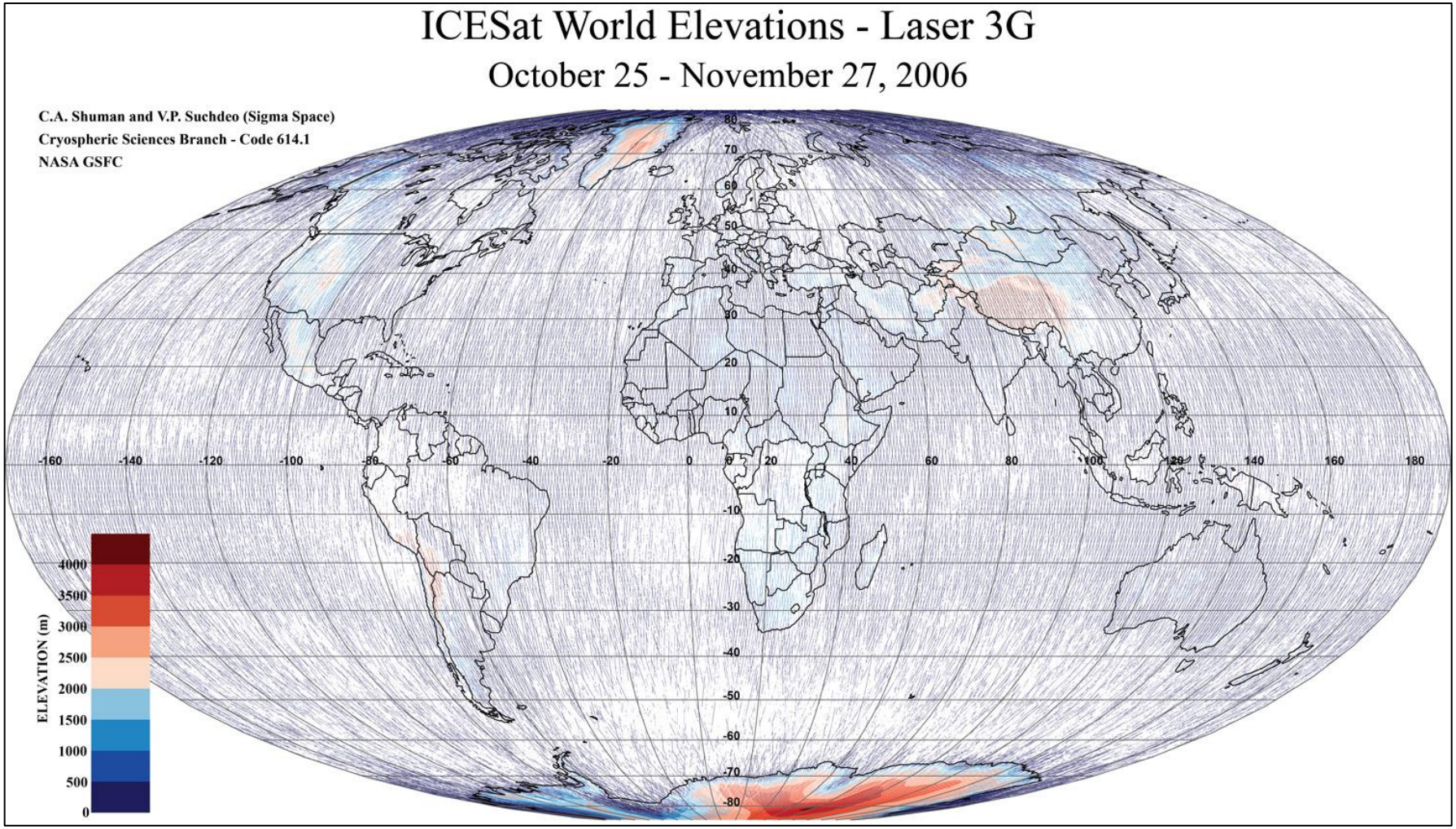
ICESat World Elevations - Laser 3G
October 25 - November 27, 2006
C.A. Shuman and V.P. Suchdeo (Sigma Space)
Cryospheric Sciences Branch - Code 614.1
NASA GSFC
ELEVATION (m)
4000
3500
3000
2500
2000
1500
1000
500
0

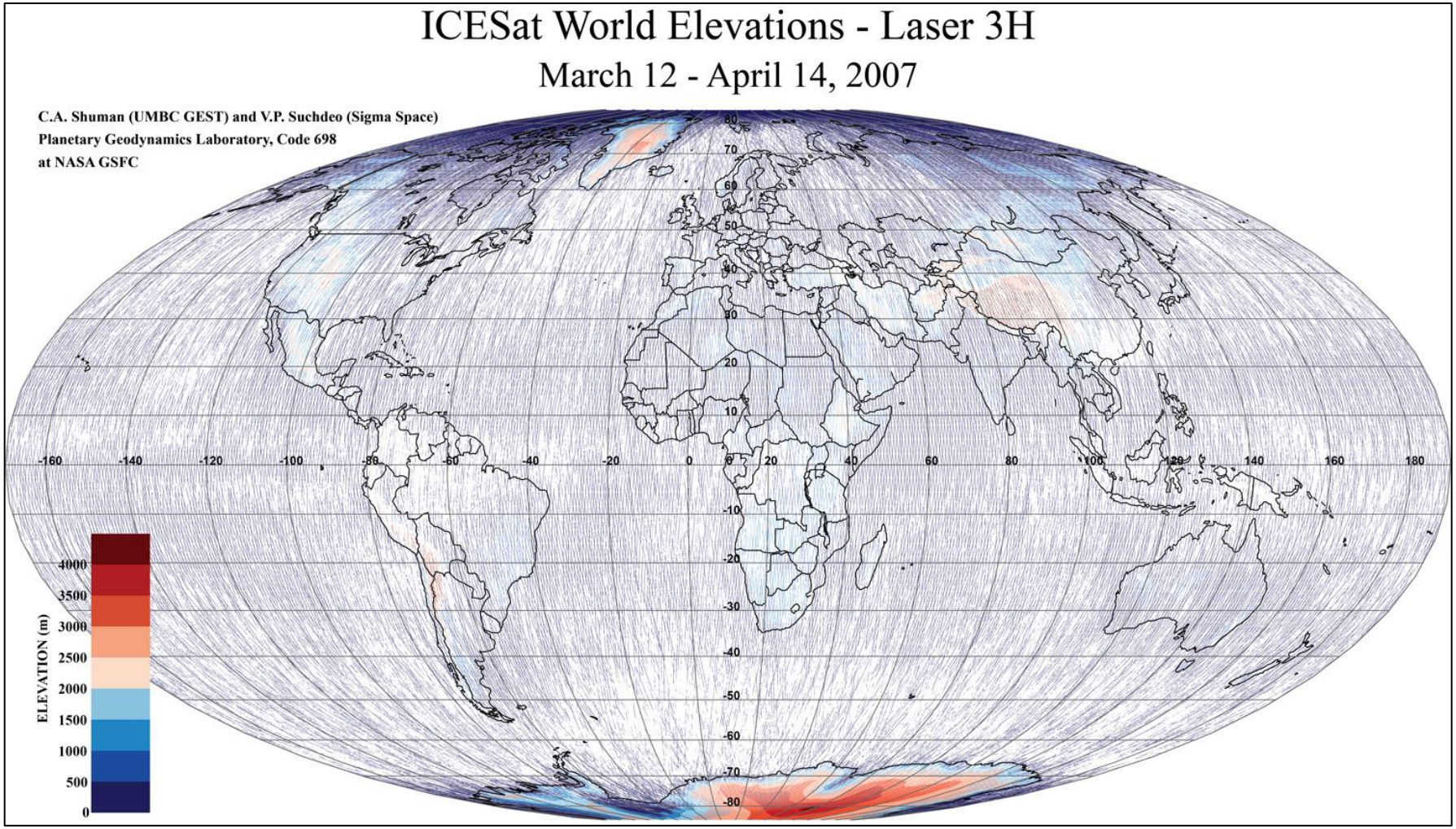
ICESat World Elevations - Laser 3H
March 12 - April 14, 2007
C.A. Shuman (UMBC GEST) and V.P. Suchdeo (Sigma Space)
Planetary Geodynamics Laboratory, Code 698
at NASA GSFC
ELEVATION (m)
4000
3500
3000
2500
2000
1500
1000
500
0

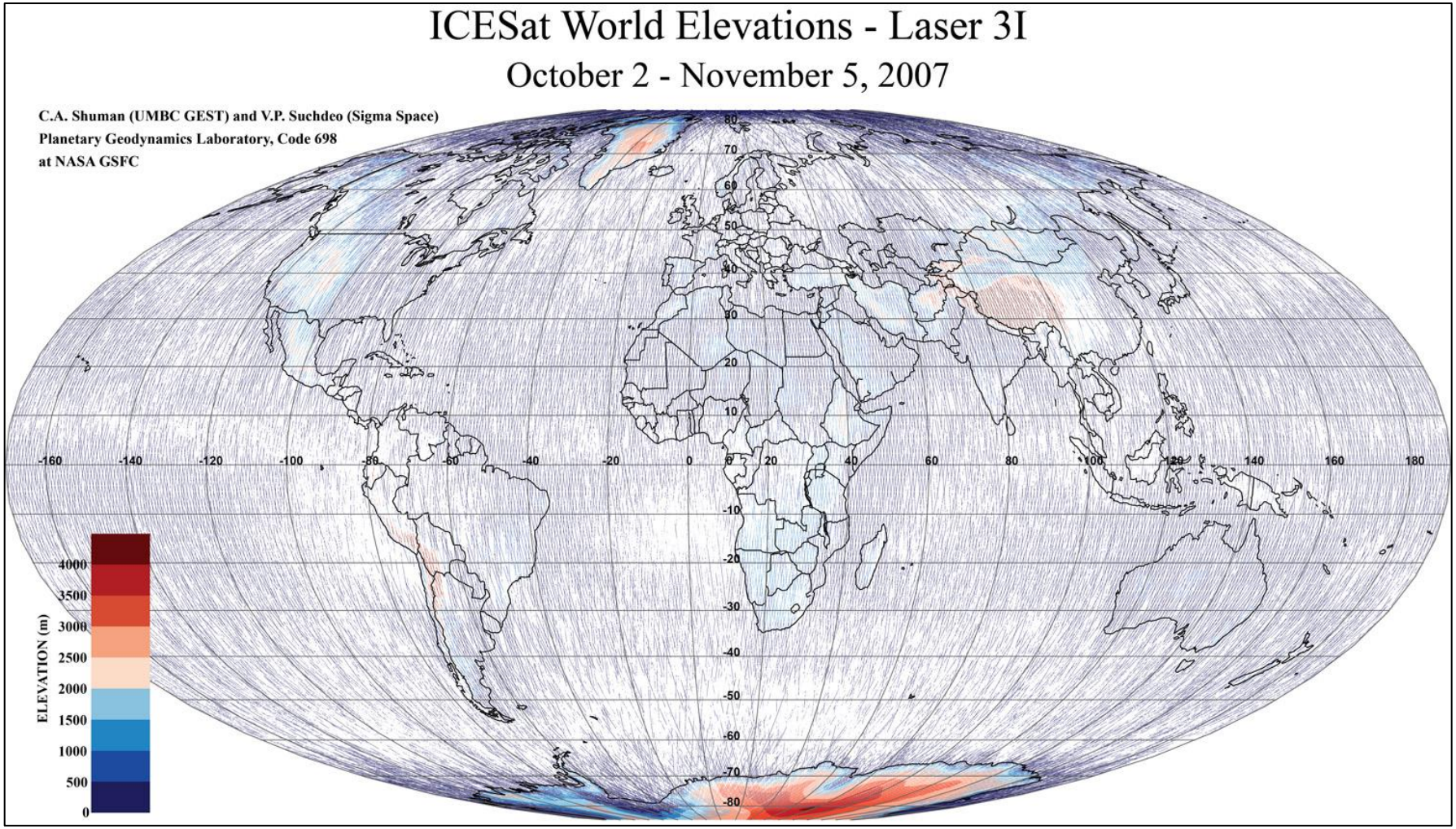
ICESat World Elevations - Laser 3I
October 2 - November 5, 2007
C.A. Shuman (UMBC GEST) and V.P. Suchdeo (Sigma Space)
Planetary Geodynamics Laboratory, Code 698
at NASA GSFC
ELEVATION (m)
4000
3500
3000
2500
2000
1500
1000
500
0

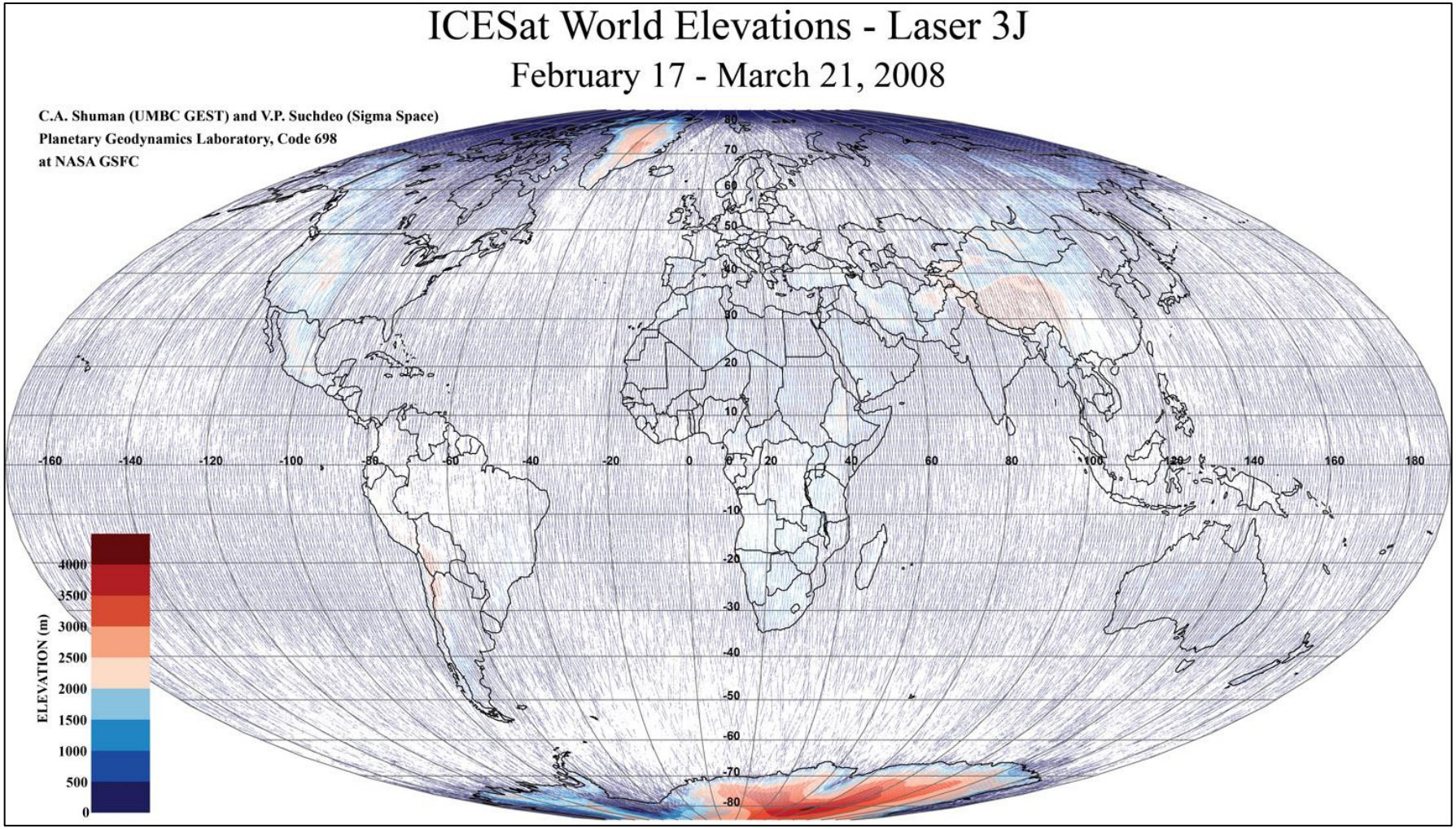
ICESat World Elevations - Laser 3J
February 17 - March 21, 2008
C.A. Shuman (UMBC GEST) and V.P. Suchdeo (Sigma Space)
Planetary Geodynamics Laboratory, Code 698
at NASA GSFC
ELEVATION (m)
4000
3500
3000
2500
2000
1500
1000
500
0

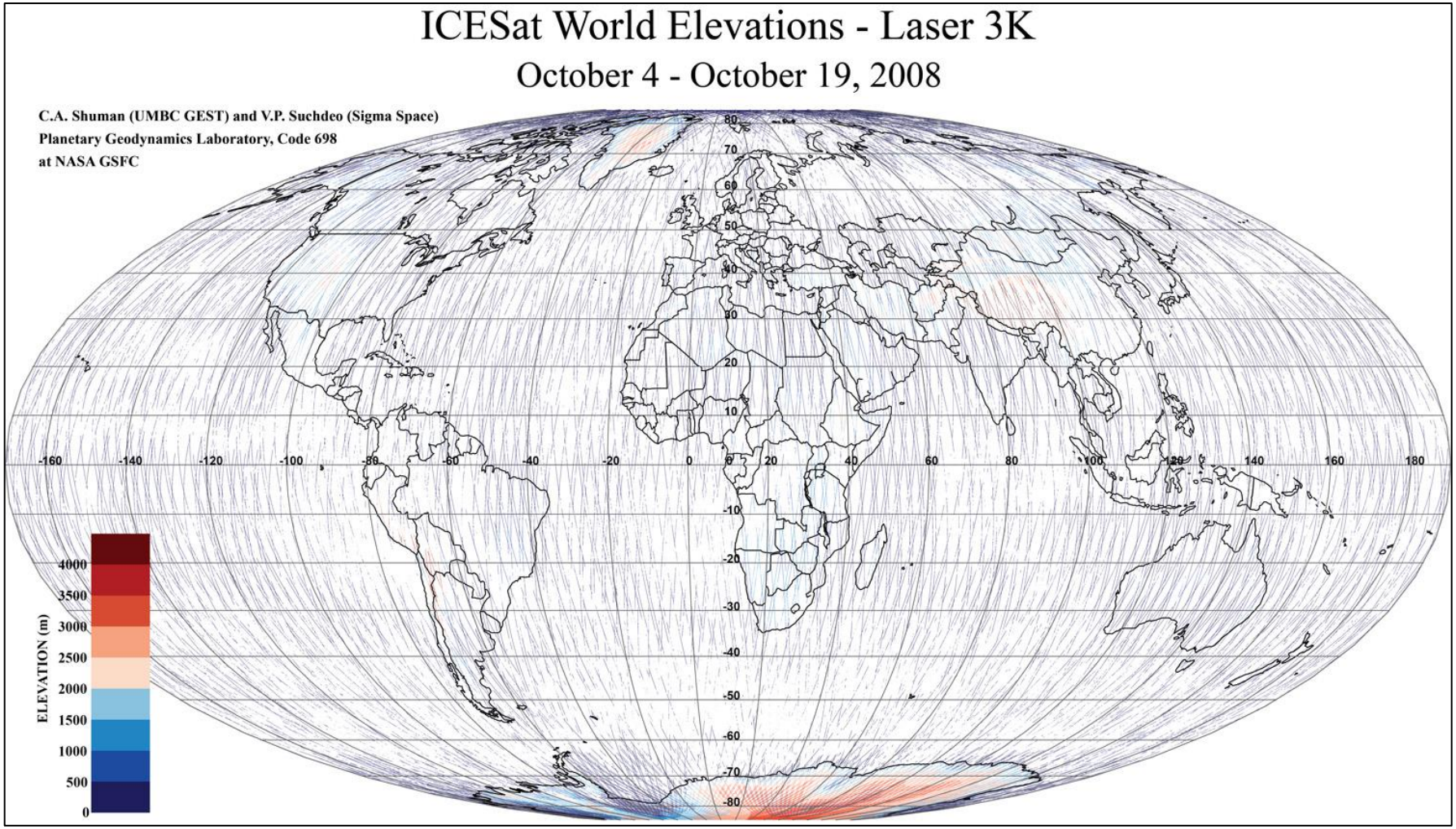
ICESat World Elevations - Laser 3K
October 4 - October 19, 2008
C.A. Shuman (UMBC GEST) and V.P. Suchdeo (Sigma Space)
Planetary Geodynamics Laboratory, Code 698
at NASA GSFC
ELEVATION (m)
4000
3500
3000
2500
2000
1500
1000
500
0

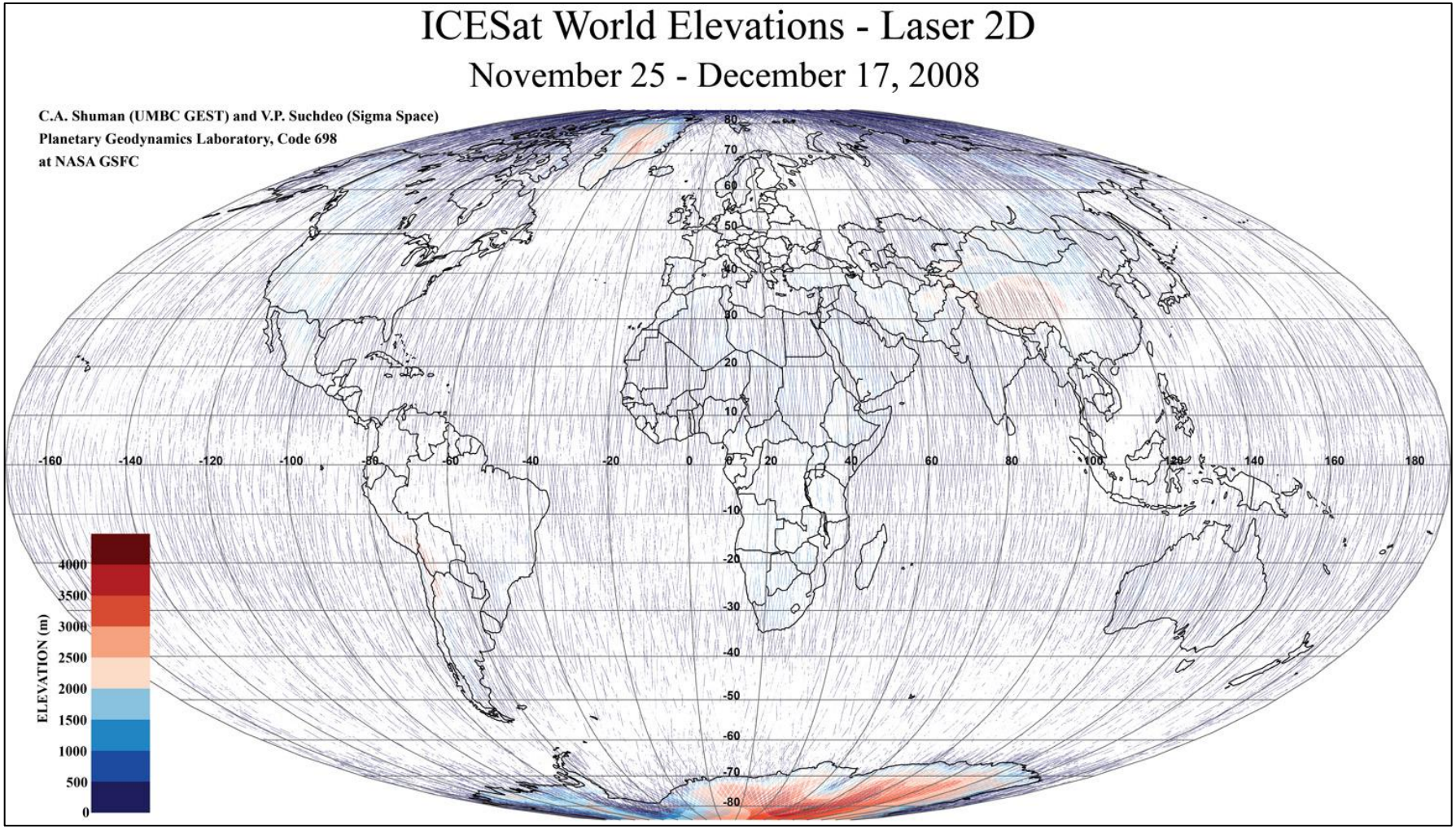
ICESat World Elevations - Laser 2D
November 25 - December 17, 2008
C.A. Shuman (UMBC GEST) and V.P. Suchdeo (Sigma Space)
Planetary Geodynamics Laboratory, Code 698
at NASA GSFC
ELEVATION (m)
4000
3500
3000
2500
2000
1500
1000
500
0
80
70
60
50
40
30
20
10
-10
-20
-30
-40
-50
-60
-70
-80
-160
-140
-120
-100
-80
-60
-40
-20
0
20
40
60
80
100
120
140
160
180

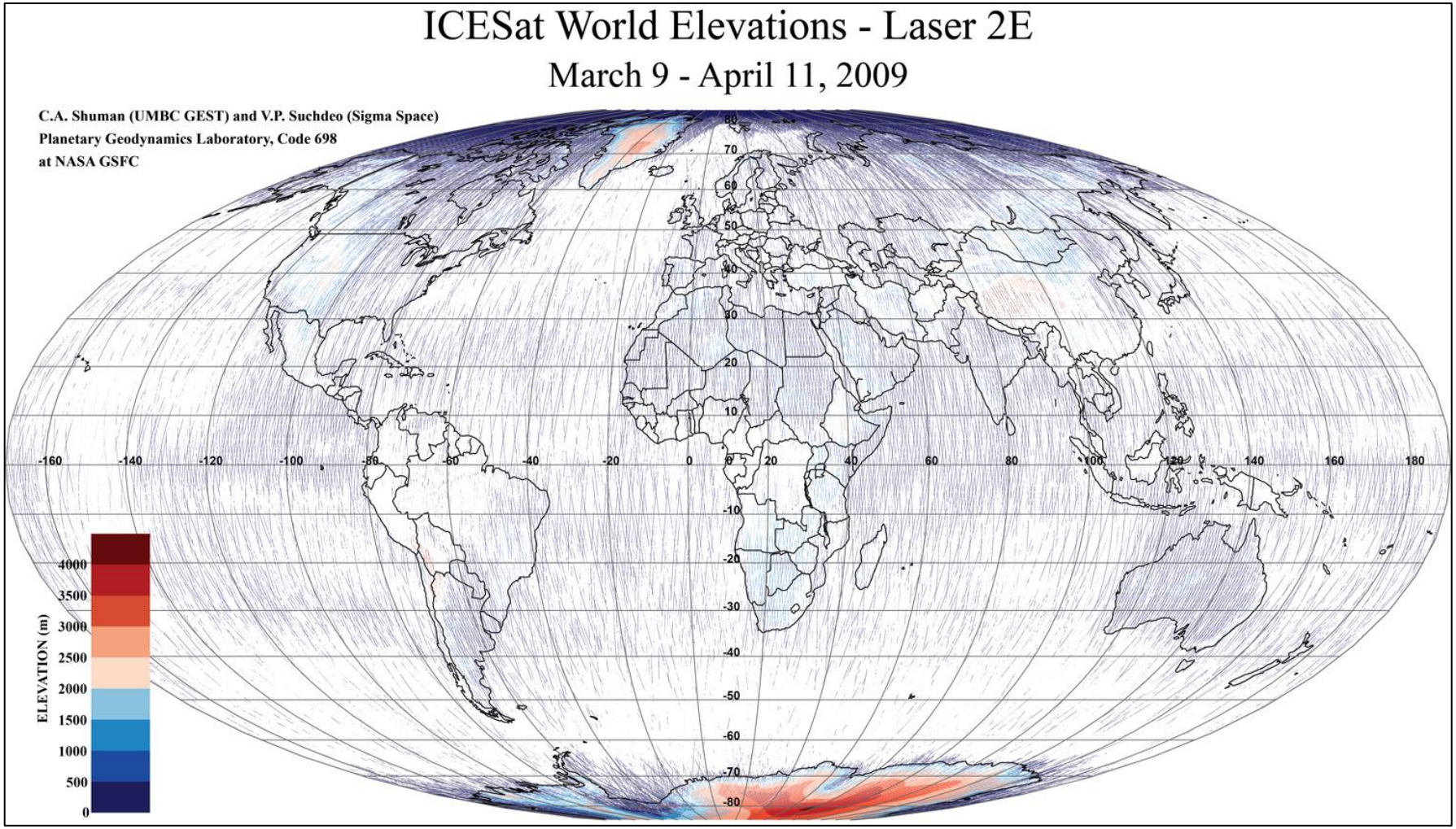
ICESat World Elevations - Laser 2E
March 9 - April 11, 2009
C.A. Shuman (UMBC GEST) and V.P. Suchdeo (Sigma Space)
Planetary Geodynamics Laboratory, Code 698
at NASA GSFC
ELEVATION (m)
4000
3500
3000
2500
2000
1500
1000
500
0

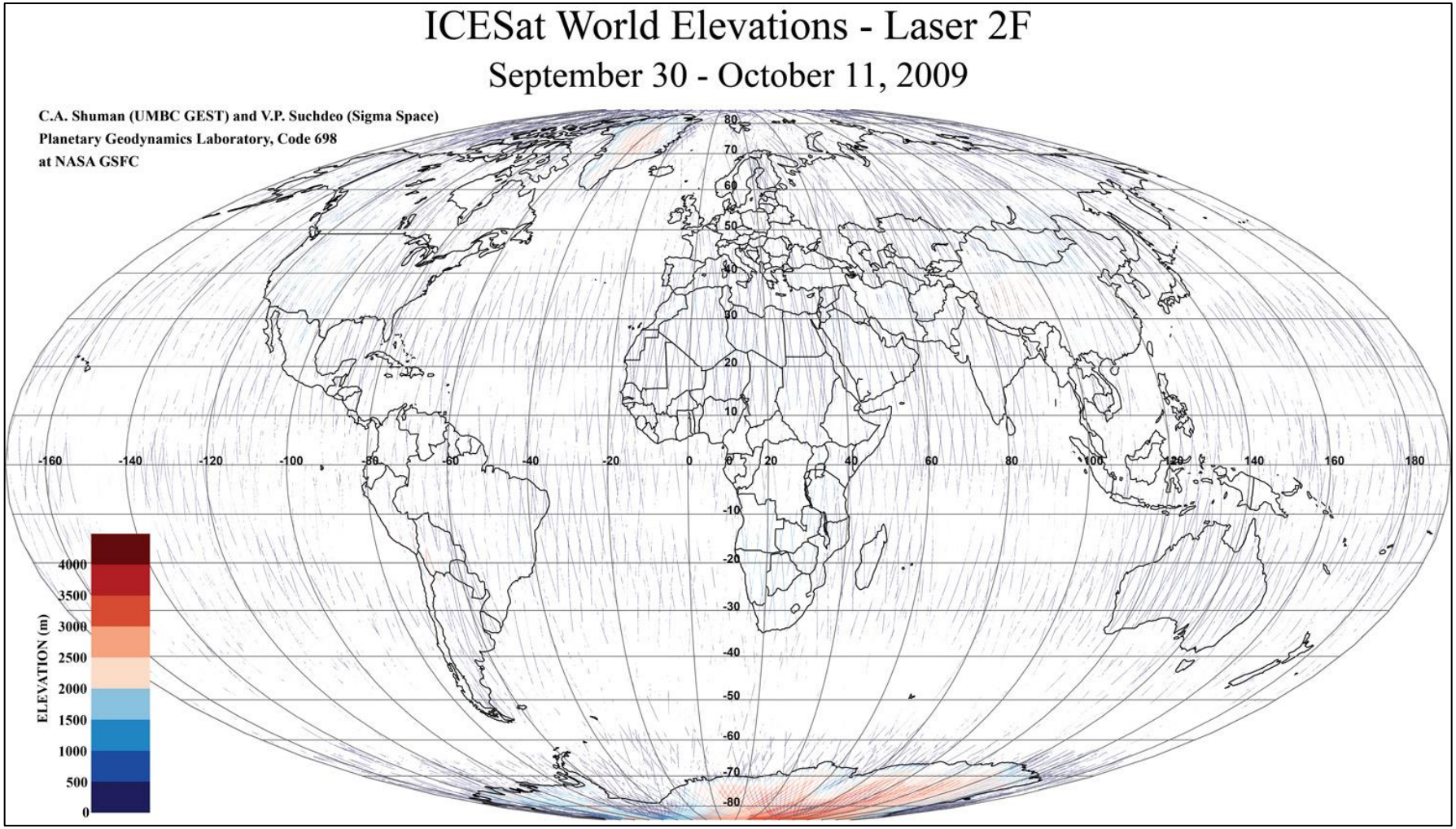
ICESat World Elevations - Laser 2F
September 30 - October 11, 2009
C.A. Shuman (UMBC GEST) and V.P. Suchdeo (Sigma Space)
Planetary Geodynamics Laboratory, Code 698
at NASA GSFC
ELEVATION (m)
4000
3500
3000
2500
2000
1500
1000
500
0
80
70
60
50
40
30
20
10
-10
-20
-30
-40
-50
-60
-70
-80
-160
-140
-120
-100
-80
-60
-40
-20
0
20
40
60
80
100
120
140
160
180

APPENDIX C: ICESAT POLAR MAPS 2

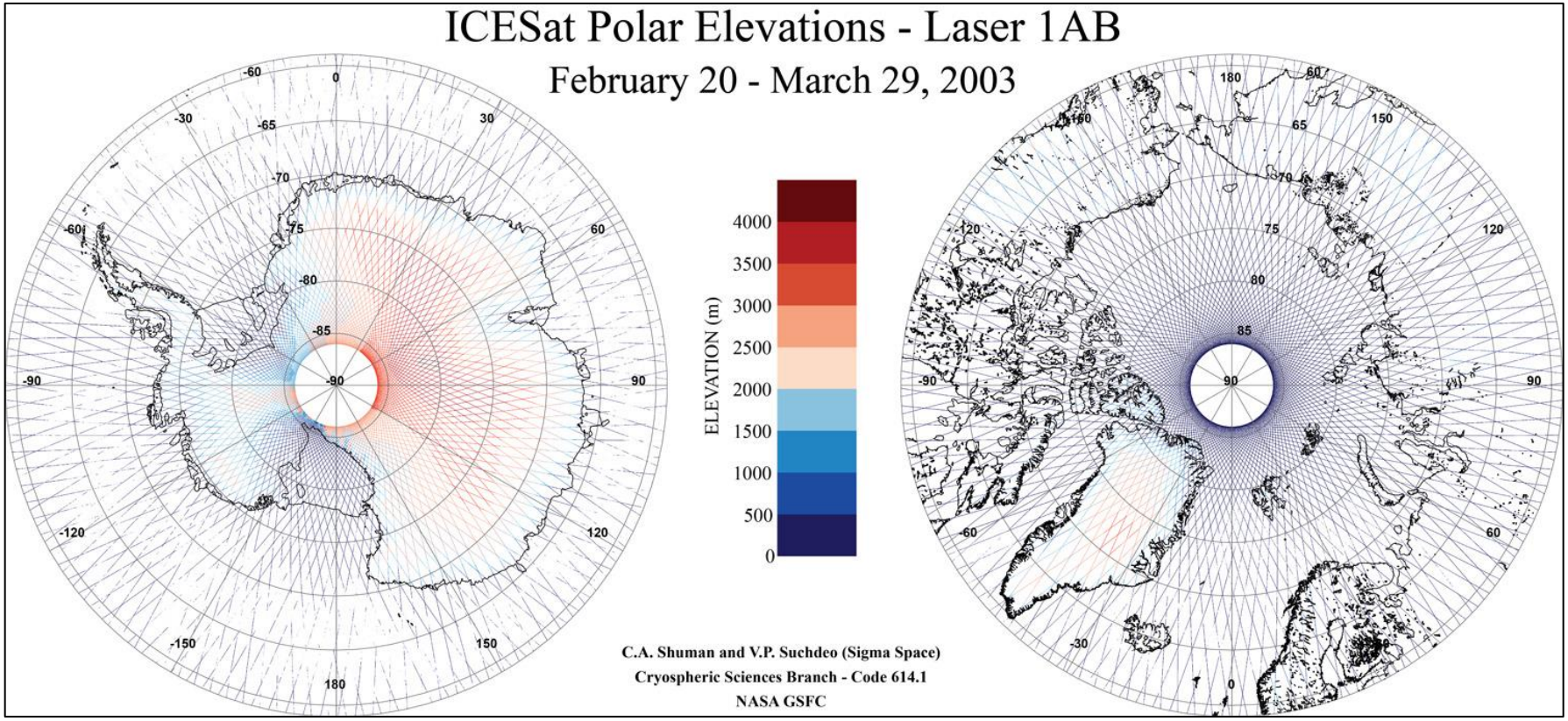

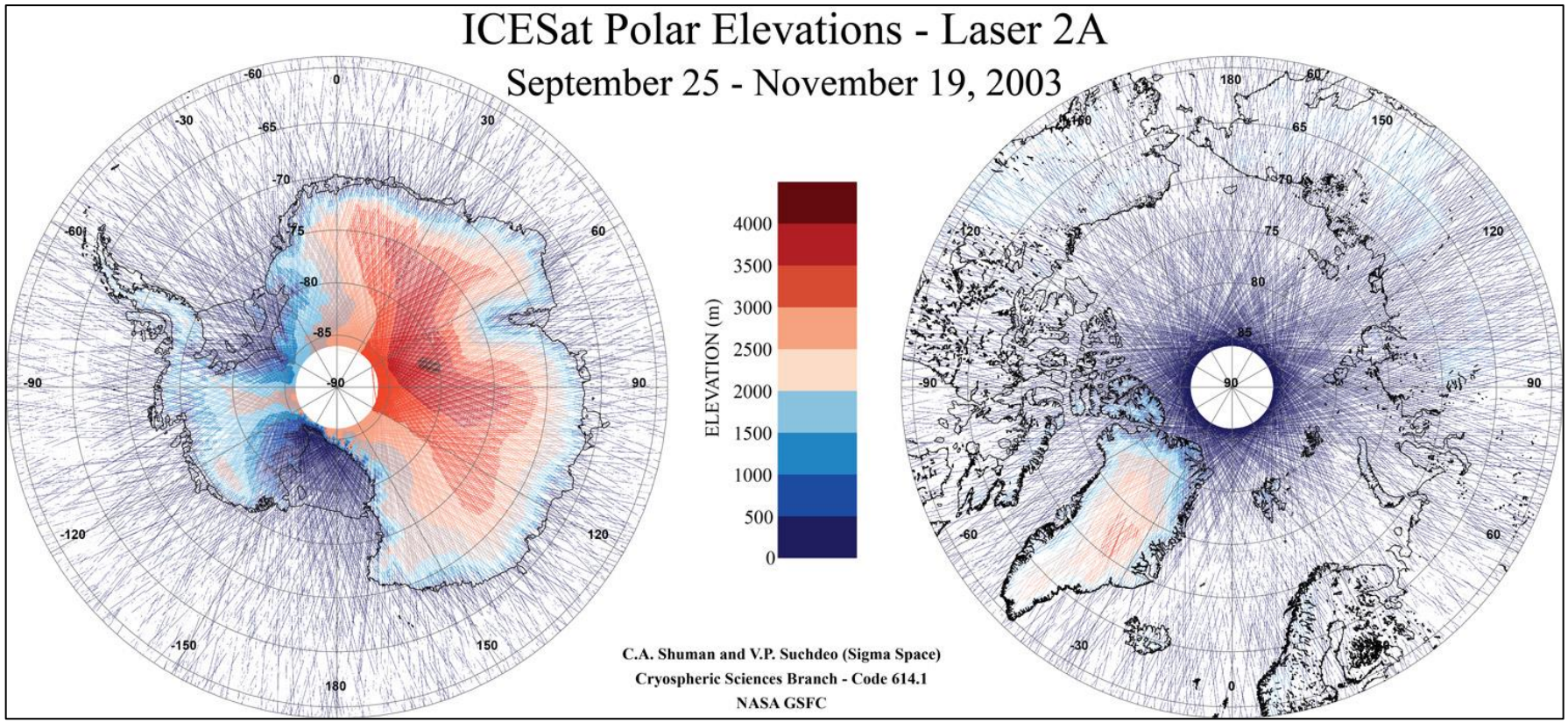
ICESat Polar Elevations - Laser 2A
September 25 - November 19, 2003
ELEVATION (m)
4000
3500
3000
2500
2000
1500
1000
500
0
C.A. Shuman and V.P. Suchdeo (Sigma Space)
Cryospheric Sciences Branch - Code 614.1
NASA GSFC

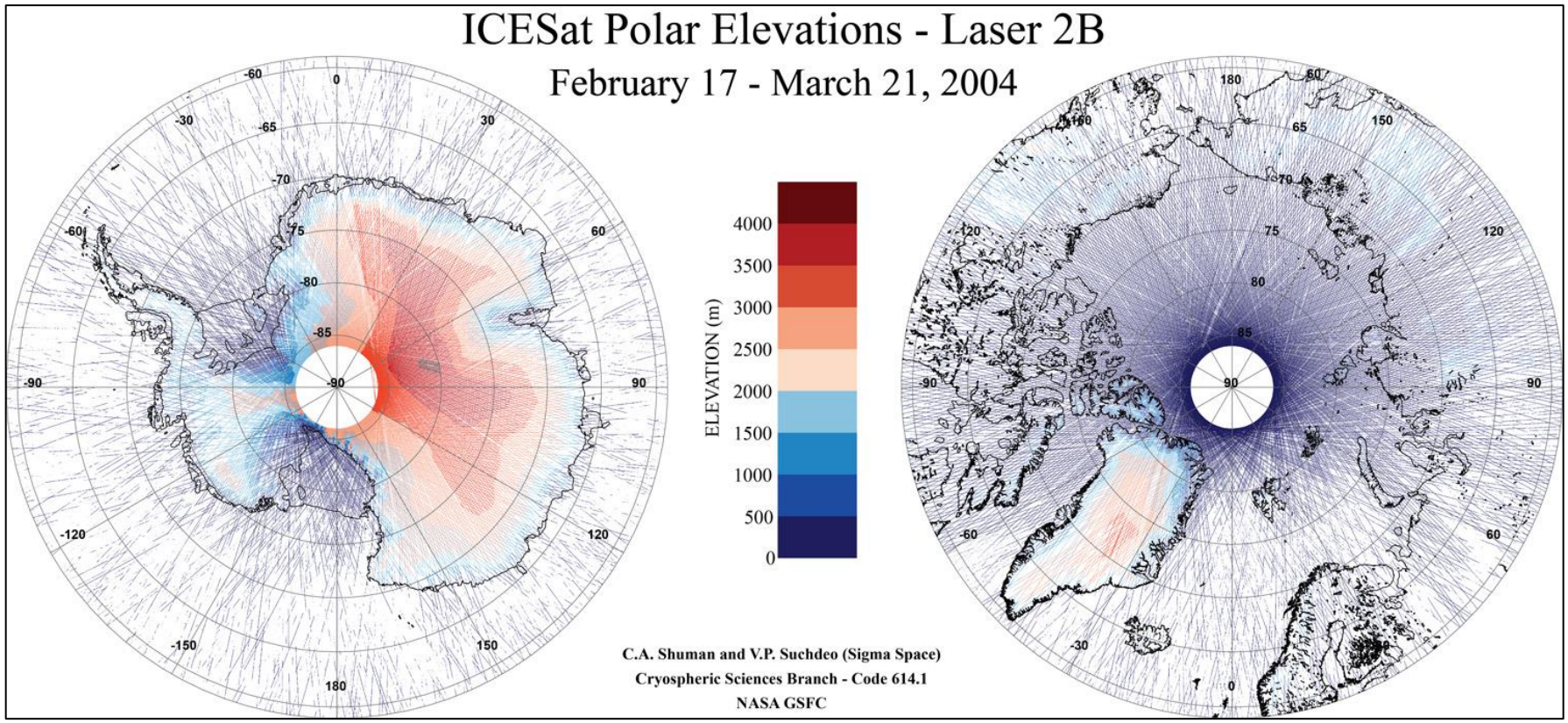
ICESat Polar Elevations - Laser 2B
February 17 - March 21, 2004
ELEVATION (m)
4000
3500
3000
2500
2000
1500
1000
500
0
C.A. Shuman and V.P. Suchdeo (Sigma Space)
Cryospheric Sciences Branch - Code 614.1
NASA GSFC

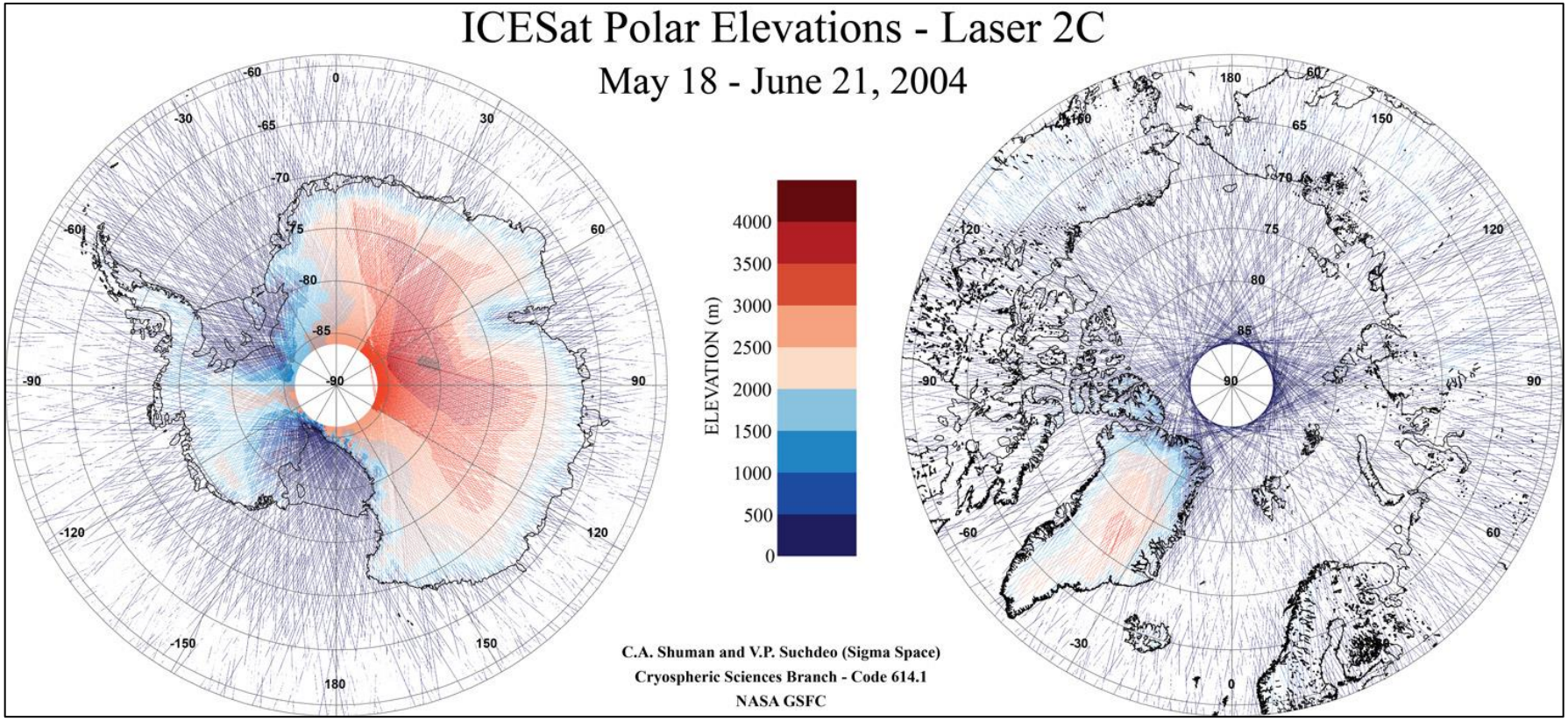
ICESat Polar Elevations - Laser 2C
May 18 - June 21, 2004
ELEVATION (m)
4000
3500
3000
2500
2000
1500
1000
500
0
C.A. Shuman and V.P. Suchdeo (Sigma Space)
Cryospheric Sciences Branch - Code 614.1
NASA GSFC

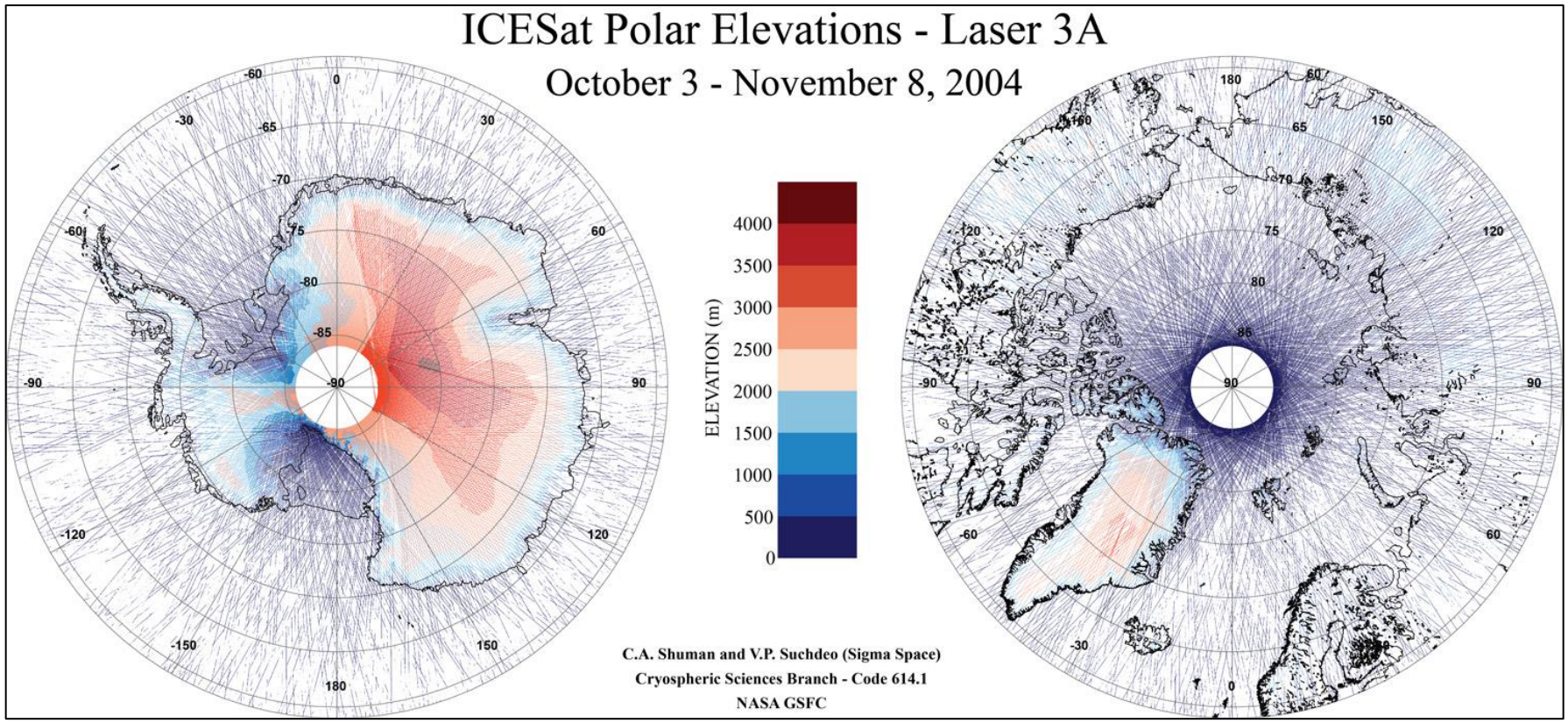
ICESat Polar Elevations - Laser 3A
October 3 - November 8, 2004
ELEVATION (m)
4000
3500
3000
2500
2000
1500
1000
500
0
C.A. Shuman and V.P. Suchdeo (Sigma Space)
Cryospheric Sciences Branch - Code 614.1
NASA GSFC

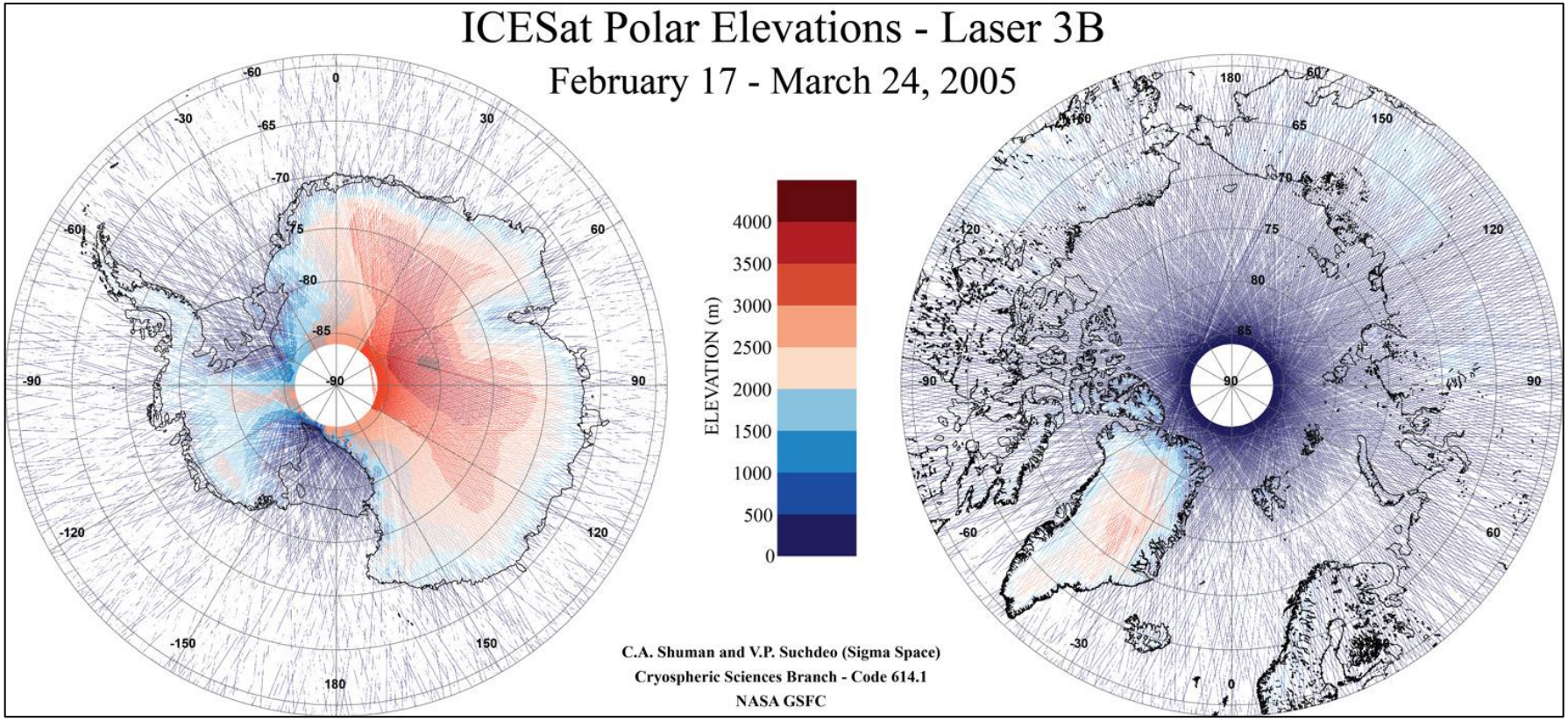
ICESat Polar Elevations - Laser 3B
February 17 - March 24, 2005
ELEVATION (m)
4000
3500
3000
2500
2000
1500
1000
500
0
C.A. Shuman and V.P. Suchdeo (Sigma Space)
Cryospheric Sciences Branch - Code 614.1
NASA GSFC

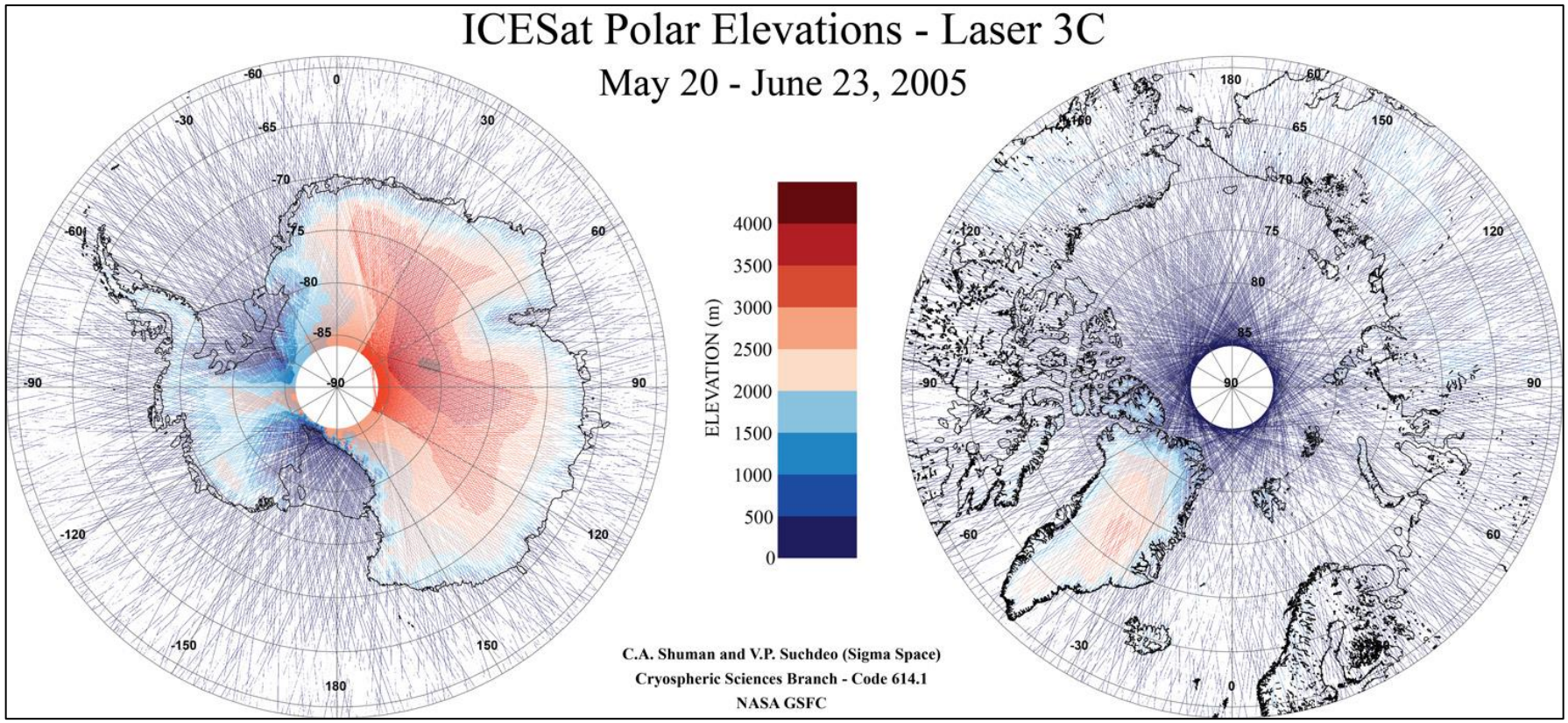
ICESat Polar Elevations - Laser 3C
May 20 - June 23, 2005
ELEVATION (m)
4000
3500
3000
2500
2000
1500
1000
500
0
C.A. Shuman and V.P. Suchdeo (Sigma Space)
Cryospheric Sciences Branch - Code 614.1
NASA GSFC

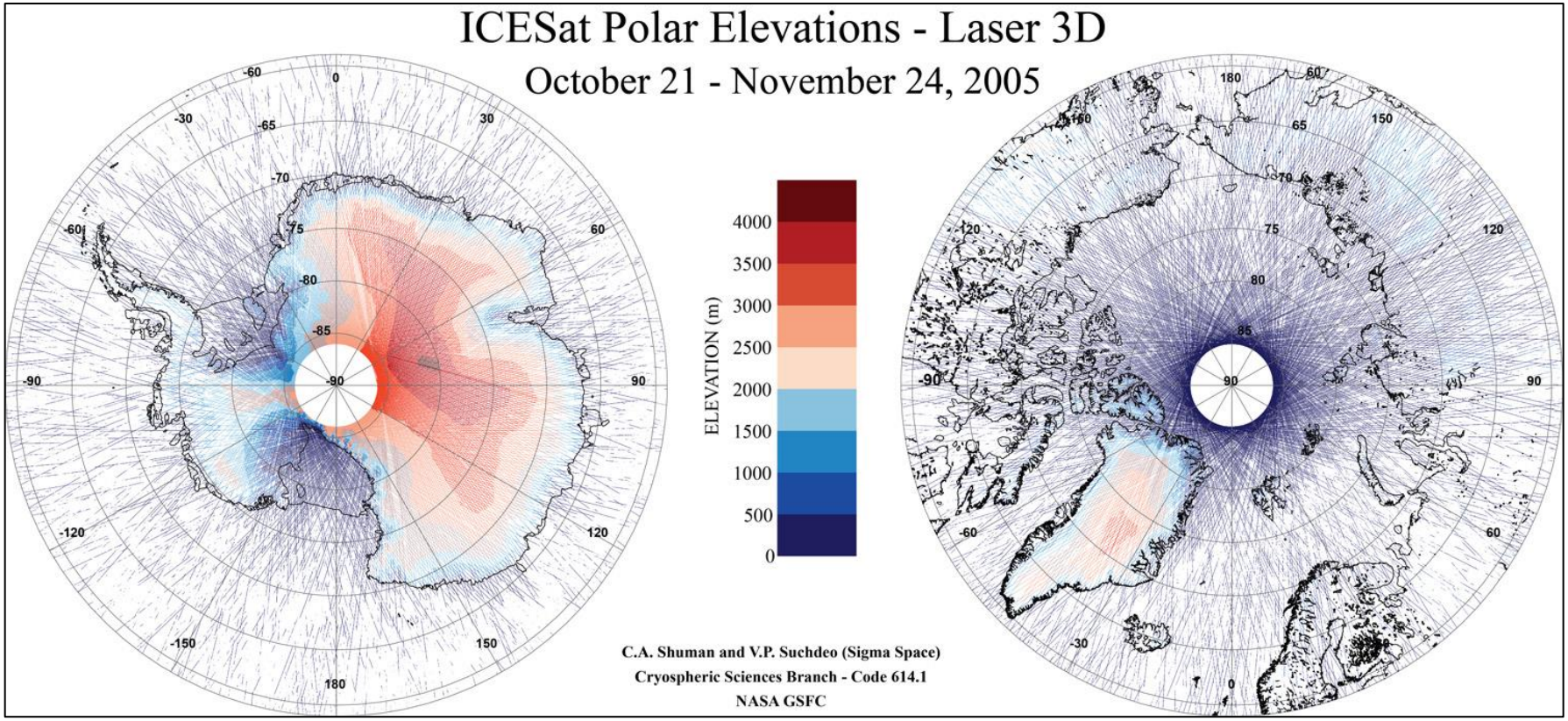
ICESat Polar Elevations - Laser 3D
October 21 - November 24, 2005
ELEVATION (m)
4000
3500
3000
2500
2000
1500
1000
500
0
C.A. Shuman and V.P. Suchdeo (Sigma Space)
Cryospheric Sciences Branch - Code 614.1
NASA GSFC

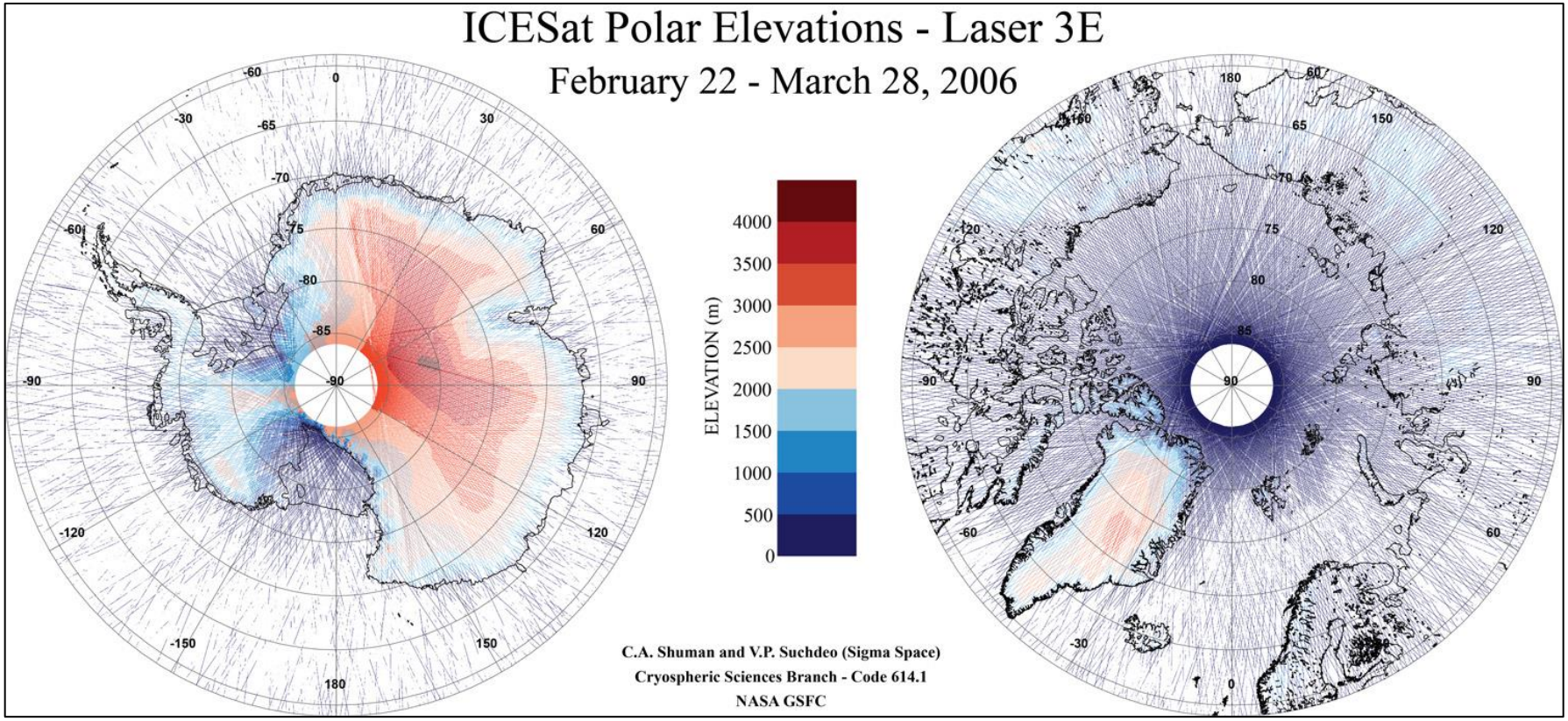
ICESat Polar Elevations - Laser 3E
February 22 - March 28, 2006
ELEVATION (m)
4000
3500
3000
2500
2000
1500
1000
500
0
C.A. Shuman and V.P. Suchdeo (Sigma Space)
Cryospheric Sciences Branch - Code 614.1
NASA GSFC

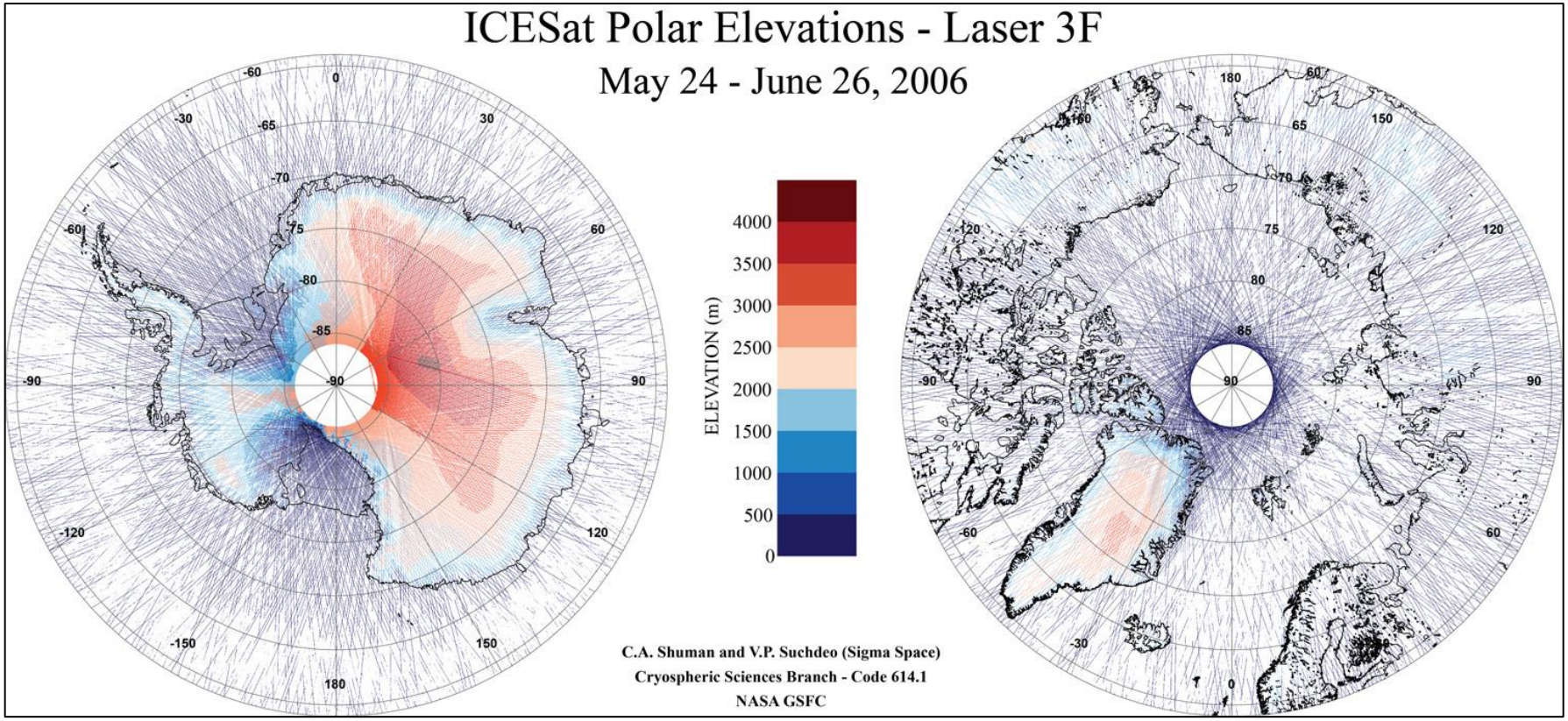
ICESat Polar Elevations - Laser 3F
May 24 - June 26, 2006
ELEVATION (m)
4000
3500
3000
2500
2000
1500
1000
500
0
C.A. Shuman and V.P. Suchdeo (Sigma Space)
Cryospheric Sciences Branch - Code 614.1
NASA GSFC

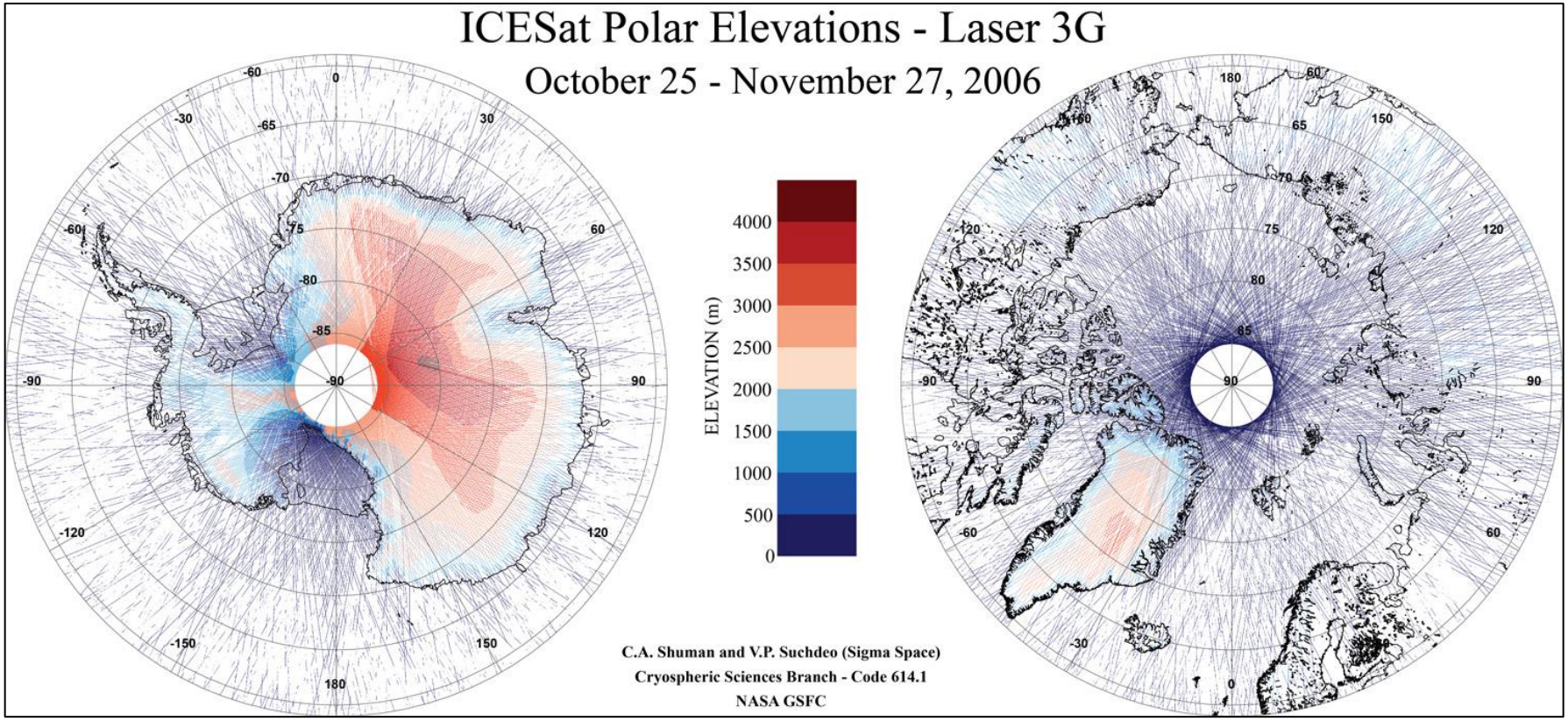
ICESat Polar Elevations - Laser 3G
October 25 - November 27, 2006
ELEVATION (m)
4000
3500
3000
2500
2000
1500
1000
500
0
C.A. Shuman and V.P. Suchdeo (Sigma Space)
Cryospheric Sciences Branch - Code 614.1
NASA GSFC

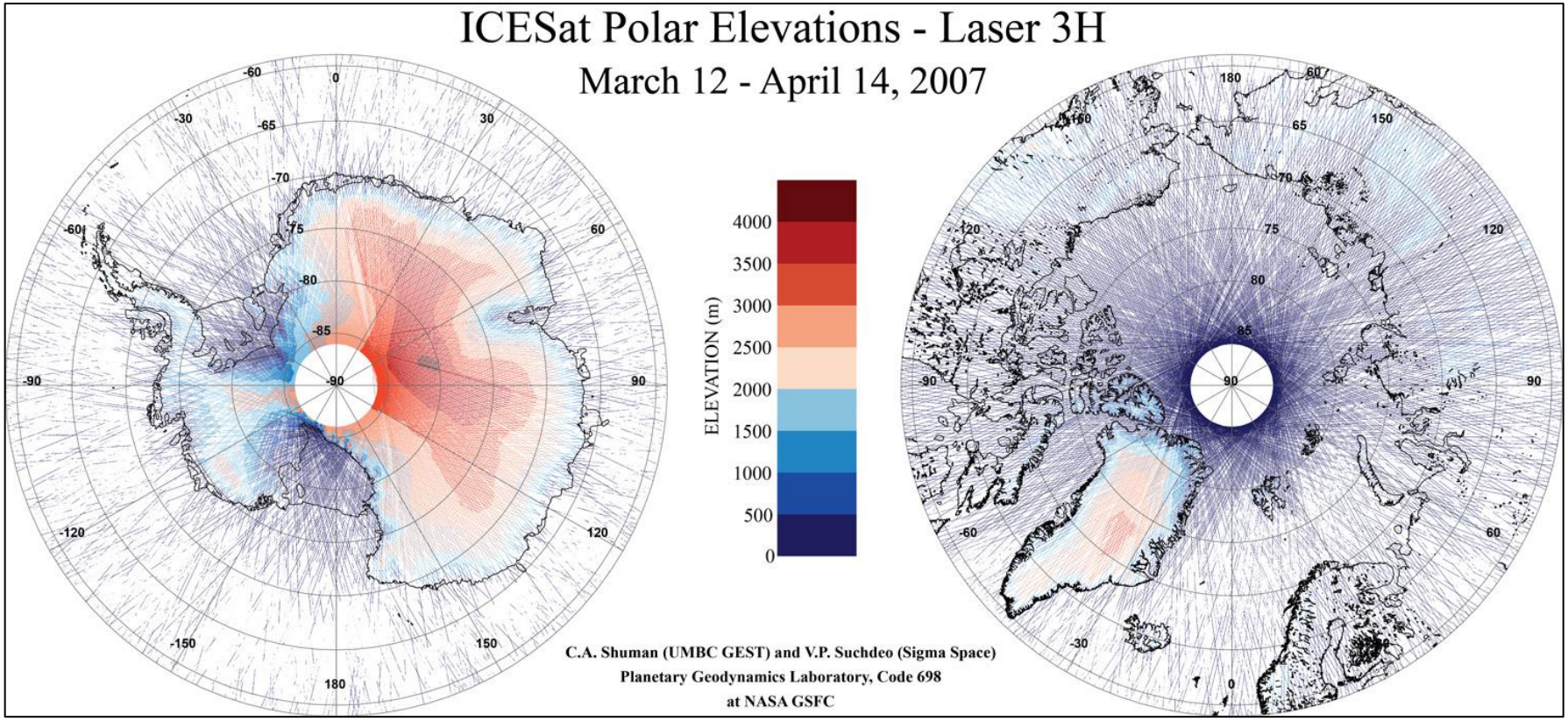
ICESat Polar Elevations - Laser 3H
March 12 - April 14, 2007
ELEVATION (m)
4000
3500
3000
2500
2000
1500
1000
500
0
C.A. Shuman (UMBC GEST) and V.P. Suchdeo (Sigma Space)
Planetary Geodynamics Laboratory, Code 698
at NASA GSFC

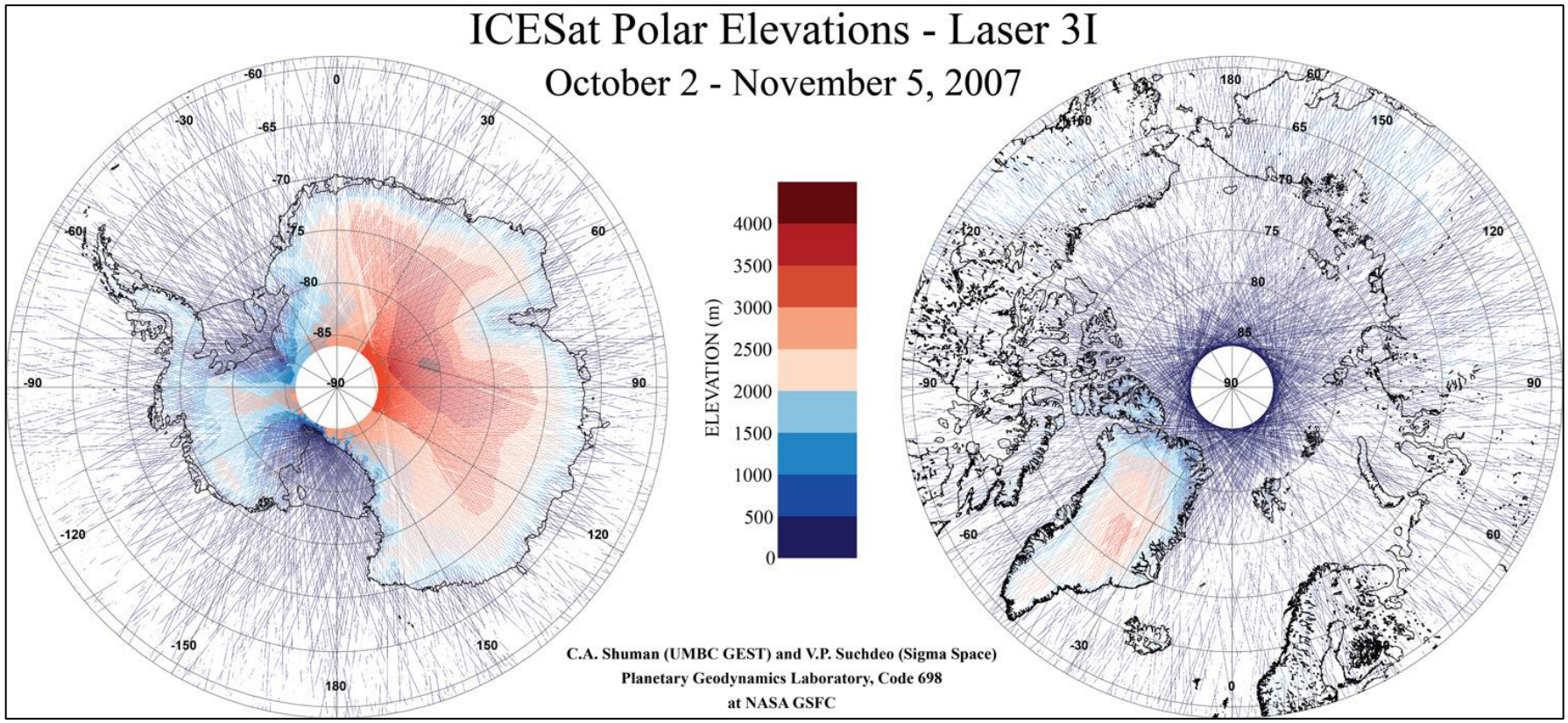
ICESat Polar Elevations - Laser 3I
October 2 - November 5, 2007
ELEVATION (m)
4000
3500
3000
2500
2000
1500
1000
500
0
C.A. Shuman (UMBC GEST) and V.P. Suchdeo (Sigma Space)
Planetary Geodynamics Laboratory, Code 698
at NASA GSFC

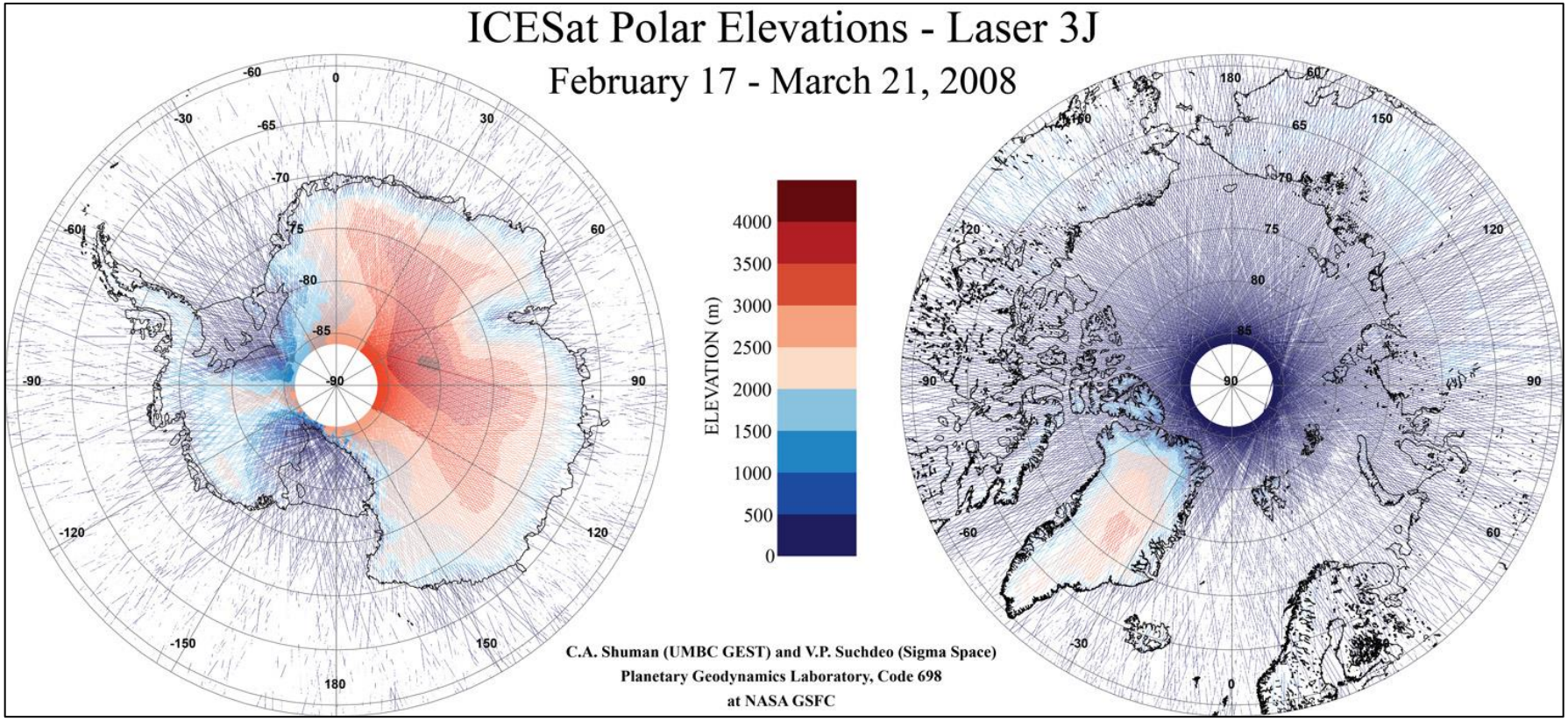
ICESat Polar Elevations - Laser 3J
February 17 - March 21, 2008
ELEVATION (m)
4000
3500
3000
2500
2000
1500
1000
500
0
C.A. Shuman (UMBC GEST) and V.P. Suchdeo (Sigma Space)
Planetary Geodynamics Laboratory, Code 698
at NASA GSFC

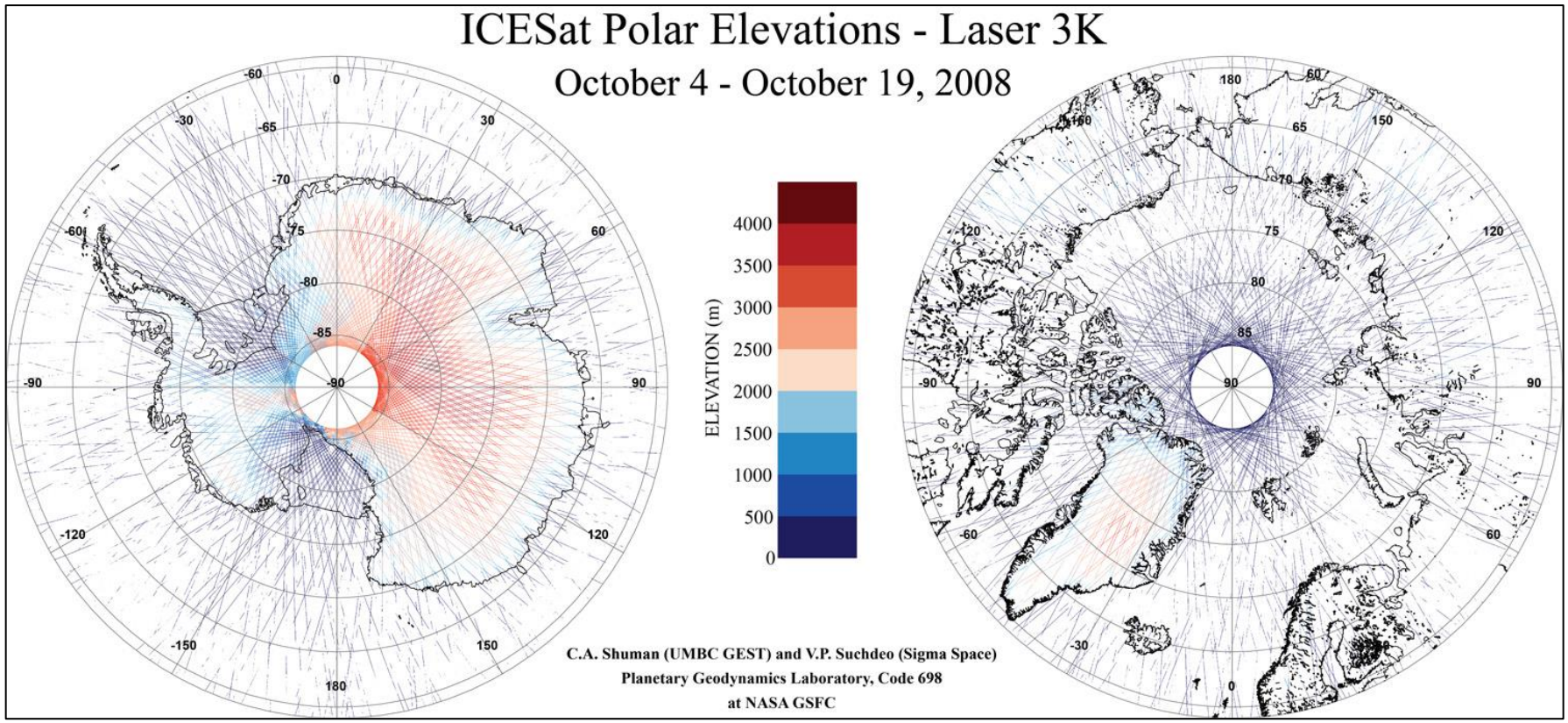
ICESat Polar Elevations - Laser 3K
October 4 - October 19, 2008
ELEVATION (m)
4000
3500
3000
2500
2000
1500
1000
500
0
C.A. Shuman (UMBC GEST) and V.P. Suchdeo (Sigma Space)
Planetary Geodynamics Laboratory, Code 698
at NASA GSFC

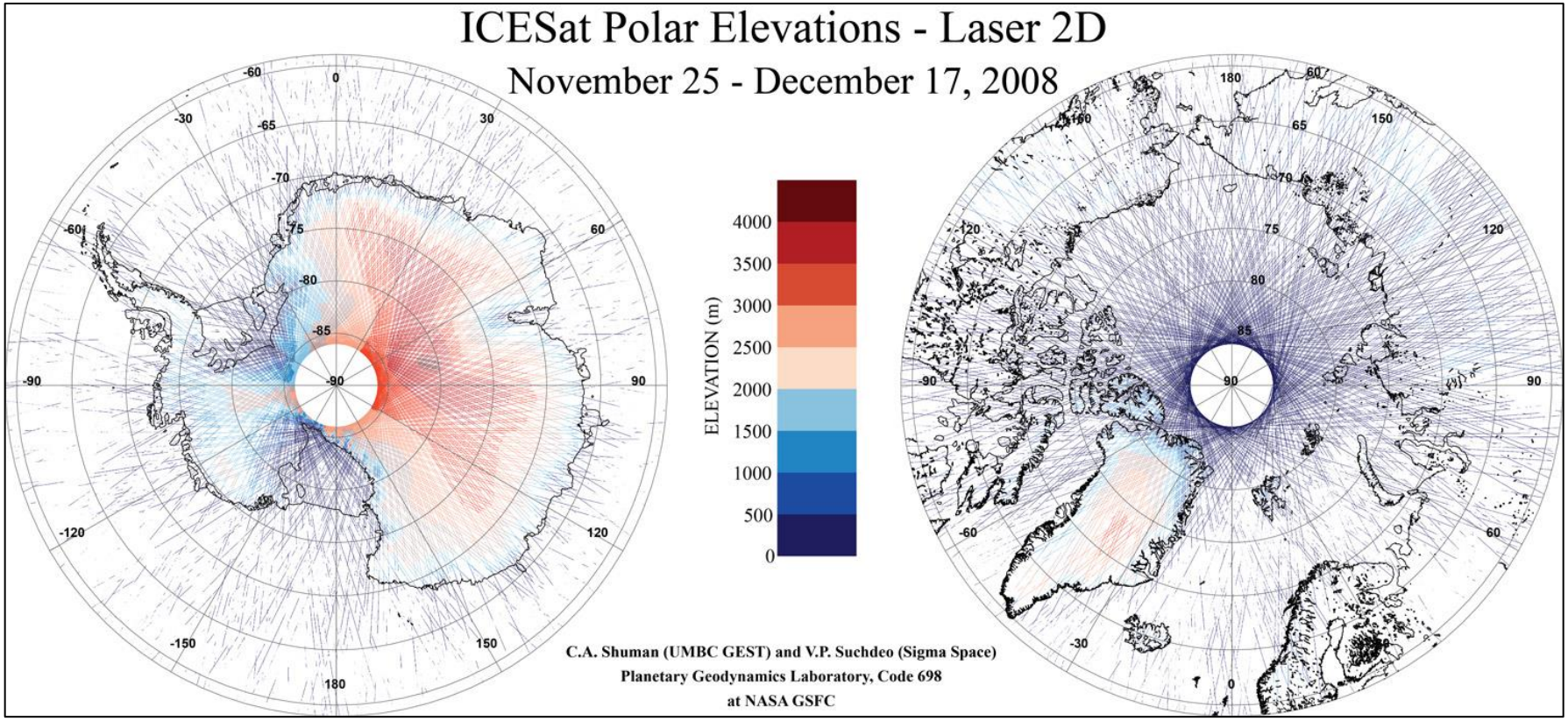
ICESat Polar Elevations - Laser 2D
November 25 - December 17, 2008
ELEVATION (m)
4000
3500
3000
2500
2000
1500
1000
500
0
C.A. Shuman (UMBC GEST) and V.P. Suchdeo (Sigma Space)
Planetary Geodynamics Laboratory, Code 698
at NASA GSFC

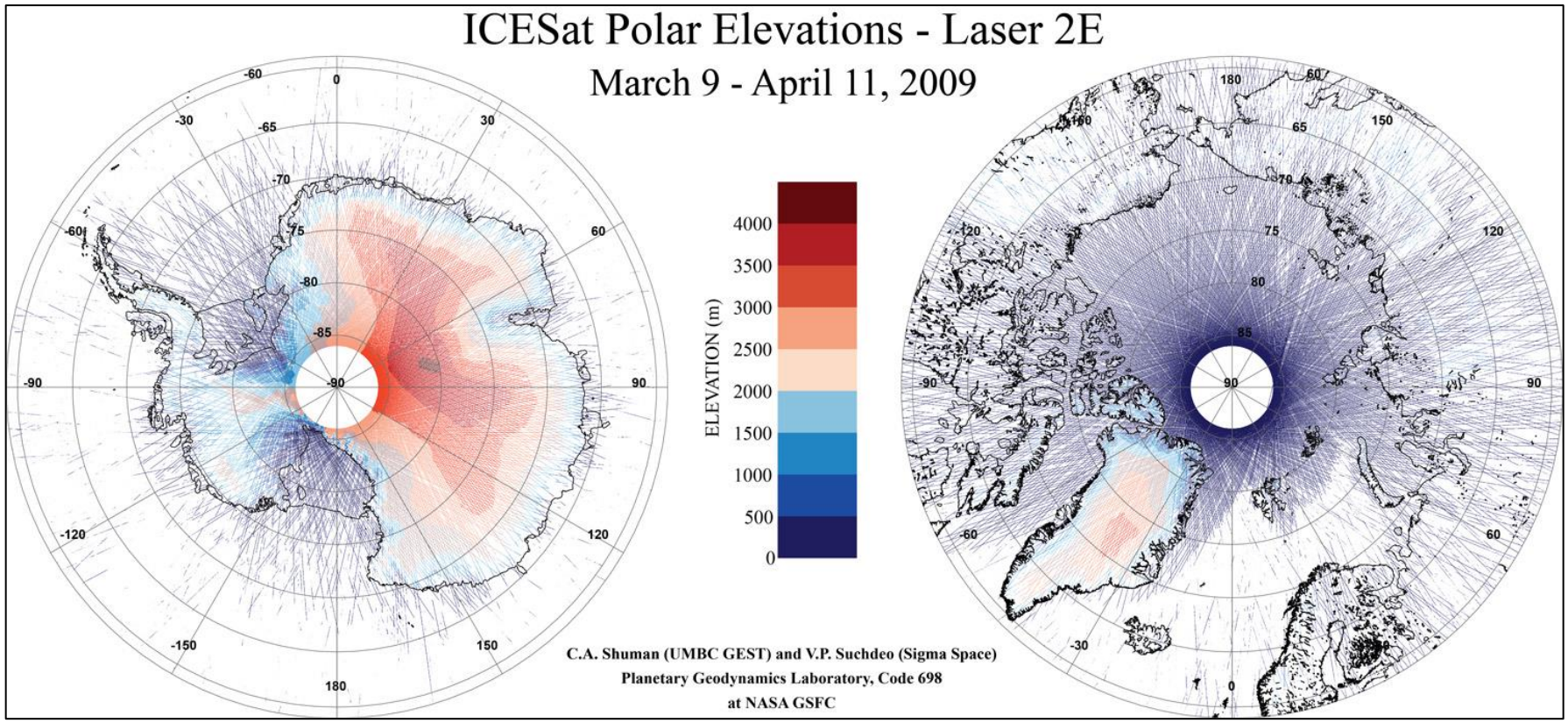
ICESat Polar Elevations - Laser 2E
March 9 - April 11, 2009
ELEVATION (m)
4000
3500
3000
2500
2000
1500
1000
500
0
C.A. Shuman (UMBC GEST) and V.P. Suchdeo (Sigma Space)
Planetary Geodynamics Laboratory, Code 698
at NASA GSFC

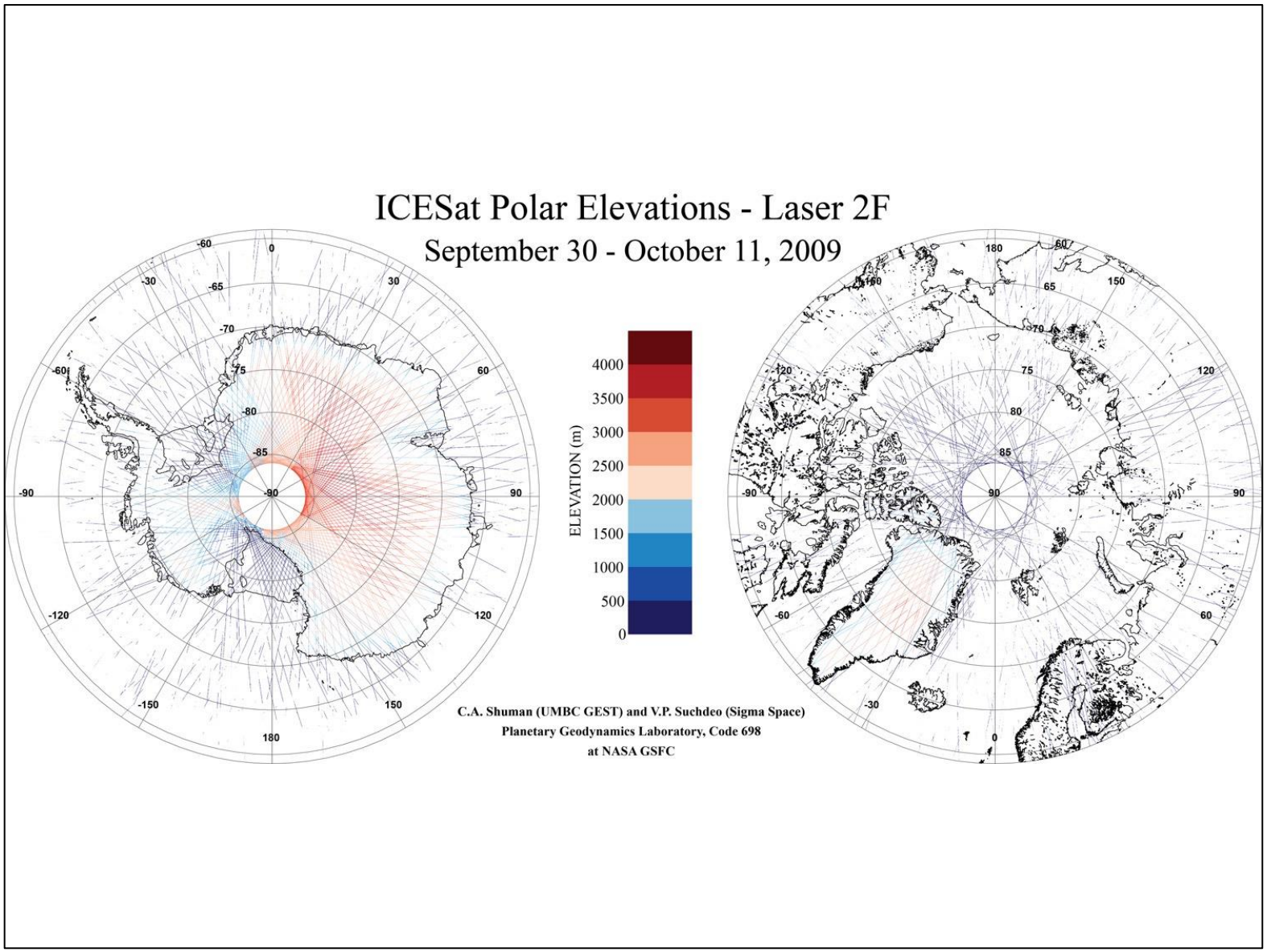
ICESat Polar Elevations - Laser 2F
September 30 - October 11, 2009
ELEVATION (m)
4000
3500
3000
2500
2000
1500
1000
500
0
C.A. Shuman (UMBC GEST) and V.P. Suchdeo (Sigma Space)
Planetary Geodynamics Laboratory, Code 698
at NASA GSFC